ABSTRACT

Title of Document: PRICING VOLATILITY DERIVATIVES USING SPACE SCALED LÉVY PROCESSES.

Samvit Prakash, Doctor of Philosophy, 2008

Directed By: Prof. Dilip B. Madan, Department of Finance
and
Prof. Tobias von Petersdorff, Department of Mathematics

The VIX index measures the one-month risk-neutral forward volatility of the S&P500 (SPX) index. While Lévy processes such as the CGMY process can price options on the underlying stock or index, they implicitly assume a constant forward volatility. This makes them unsuitable for pricing options on VIX. We propose a model within the one dimensional Markovian framework for pricing VIX and SPX options. We introduce space dependence of volatility by scaling the CGMY process with a leverage function. The resultant process can consistently price options on SPX and VIX of a given maturity. We also perform surface calibrations of options on the two indices separately. We explore the properties of the implied distribution of the SPX from both indices and conclude that the VIX index under-weighs small jumps as compared to large jumps as well as the skewness of the SPX index .

PRICING VOLATILITY DERIVATIVES USING SPACE SCALED LÉVY PROCESSES

By

Samvit Prakash

Dissertation submitted to the Faculty of the Graduate School of the
University of Maryland, College Park, in partial fulfillment
of the requirements for the degree of
Doctor of Philosophy
2008

Advisory Committee:
Professor Dilip B. Madan, Chair
Professor Tobias von Petersdorff, Co-chair
Professor Frank Alt
Professor Steve Heston
Professor Mark Loewenstein
Professor John E. Osborn

Dedication

To the first single-celled organism to which I owe my existence.

Acknowledgements

This is going to be a long list! It has to start with my advisors, Professor Dilip B. Madan and Prof. Tobias von Petersdorff. They have both gone out of their way to help and advise me. They have met with me late in the evenings after work, on weekends, and even in different cities to help me with my research. Their sharp intellect and their passion for research will always be an inspiration to me. I have benefitted tremendously from their vast knowledge, and it has been an absolute delight working with them.

I have had the good fortune of being in the company of great friends at the University of Maryland. I would especially like to thank George Panayatov for always being there as a sounding board for ideas, Jun Wang for helping me with a crucial step in the calibration algorithm, Franklin Gavilanez for his help with the dissertation typesetting, and Huaqiang (Richard) Ma, Anshuman Sinha, Niranjan Ramachandran and Domenico Nepolatani, for their friendship and favors. I would also like to thank all the members the Informal Math Finance (IMF) Discussion Group and the Math Finance RIT for many meaningful discussions on the subject.

I would like to thank my defense committee members, Professors Frank Alt, Steve Heston, Mark Loewenstein and John Osborn for taking time out to be on the committee. I would also like to thank Prof. Konstantina Trivisa and Alverda McCoy from the AMSC department for their support and encouragement throughout.

My family has been behind me throughout my adventure, often sacrificing what was important to them for my studies. I cannot thank them enough. My wife, Shivani, to

whom I owe my greatest debt, has always been with me through the best and the worst. Nothing would have been possible (or indeed meaningful) without her.

Finally, I would like to thank some unusual stars: the math department soccer team for giving me a new love in life and the staff at Ten Ren's Tea Time and their Iced Green Bubble Tea - my elixir through my grueling years in College Park!

Contents

List of Tables

List of Figures

Chapter 1

Introduction and Background

1.1 Introduction

The VIX index measures the one-month risk-neutral forward volatility of the S&P500 (SPX) index. While Lévy processes, such as the CGMY process, can price options on the underlying stock or index for a given maturity, they implicitly assume a constant forward volatility due to stationarity. This makes them unsuitable for pricing options on the VIX. Options on VIX can also be used to replicate the variance swap contract, which pays the realized variance in exchange for a fixed coupon. The same contract can also be replicated using options on the SPX. These two replicating portfolios show different prices for the variance swap contract, thus introducing the possibility of arbitrage. This arbitrage can be avoided by using a consistent model for pricing options on the VIX and the SPX. We propose such a model within a one dimensional Markovian framework for pricing VIX and SPX options. We introduce space dependence of volatility by scaling the CGMY process with leverage function. Space

scaling introduces uncertainty in volatility which allows us to price options on VIX. The resultant process can consistently price options on SPX and VIX of a given maturity. We also perform surface calibrations of options on the two indices separately. We explore the properties of the implied distribution of the SPX from both indices and conclude that the VIX index under-weighs small jumps as compared to large jumps as well as skewness of the SPX index . The main difficulty we encounter is in the calculation of the (stiffness) matrix used in the computation of option prices. We devise numerical schemes to minimize the computational burden arising from this issue. Another difficulty was in calculating the volatility (VIX) function as a function of the stock price since no closed form was available. We worked around this issue by implementing a two stage numerical scheme in which we calculated the VIX function numerically in the first stage and priced options on it in the second stage.

There has been significant growth in the use of financial derivatives in the last three decades. The initial growth was led by plain vanilla derivative contracts where the payoffs were based on the level of the underlying stock price (or an index) at some time in the future. However, over time, more exotic contracts became very popular as well. Exotic contracts are contingent claims on the realized path of the underlying asset. These contracts can be customized to offer a play on any specific aspect of the stock price process. These derivative contracts are either traded over an exchange or over the counter (OTC). According to a survey by the Bank of International Settlements in 2007 [4], the derivative notionals outstanding in worldwide OTC markets are over 500 trillion dollars and over 300 trillion dollars for exchange traded derivatives (ETD) . Given the amount of activity in this area, there has been an increasing

demand for processes which can not only calibrate to the current market prices of exchange traded derivatives but also give realistic prices for more exotic derivatives. This basically translates into a demand for pricing processes with more realistic assumptions on transition probabilities and higher moments of marginal distributions of the underlying asset.

Louis Bachelier [1] sowed the seeds of financial engineering in 1900 by describing the distribution of stock prices as through a Gaussian distribution. This is consistent with modeling the stock price process as a Brownian motion. The next major breakthrough in option pricing came seven decades later from Black, Merton and Scholes (BMS) [6] and [43]. The BMS model assumed that the stock return process was one with independent and identical Gaussian increments with a constant drift. In continuous time, the stock price dynamics can be written as:

$$dS_t = \mu S_t dt + \sigma S_t dW_t \tag{1.1}$$

Here S_t is the stock process, μ is the drift of the process and σ is the instantaneous volatility of the stock. If r denotes the risk free interest rate, Black-Merton-Scholes showed that vanilla European options can be priced using r, irrespective of the level of μ. See Musiela & Rutkowski [45] and Bjork [8] for a detailed description of the BMS and the Bachelier models. Harrison & Kreps [29] and Harrison & Pliska [30] further showed that the absence of arbitrage is equivalent to the existence of a risk neutral probability measure under which the discounted asset prices are martingales. See Delbaen and Schachermayer [20] for more details.

While their work heralded the beginning of modern option pricing theory, the deficiencies of their model soon became increasingly clear. These deficiencies are very well documented in the financial literature, for instance, in the survey by Bates [5] and Bakshi, Cao and Chen [2]. Their assumptions of constant volatility and symmetric return distributions have been shown to be inconsistent with the market data. See Hull [32] for more details. The discrepancy appears both in the statistical (historical) returns data and in risk neutral distributions implied by option prices. This led to the development of two classes of models. One class focussed on modeling volatility as a stochastic process. The first model of this type was introduced by Heston [31]. Stochastic volatility models have been very popular and have become an industry standard in many asset classes like fixed income, foreign exchange and commodities. Other popular models in this class are Lewis' 3/2 model [36] and Hagan et. al.'s SABR model [28]. See Fouque, Papanicolaou & Sircar [26] for a comprehensive overview of stochastic volatility models. The other class consisted of models which jumps. The early development of jump models was in a jump-diffusion framework developed by Merton [44]. A class of models emerged later where the diffusion component was abandoned and the stock price was modeled as a pure jump process with an infinite activity of small jumps in an arbitrary interval of time. The first such model was the Variance Gamma (VG) process, introduced by Madan and Milne [38], and Madan and Seneta [39]. The VG process belongs to the class of pure jump Lévy processes. Lévy processes are processes with independent and identical increments. In their most general form, they also have a diffusion component. We will describe them in greater detail below.

The VG process was generalized by Carr, Madan and Chang [13] to allow for non symmetric return distributions. Carr, Geman, Madan and Yor [10] later generalized the VG process to also allow for infinite variation of the return process. The new process, which became known as the CGMY process [10] after the authors' initials, has a parameter which governs the properties of finite or infinite variation. Being a Lévy process, the CGMY process also has stationary and independent increments. We will discuss the CGMY process in detail below. Other popular models in the class of Levy processes are the Meixner process by Schoutens [51], the Generalized Hyperbolic model by Eberlein, Keller & Prause [24], Barndorff-Nielen's Normal Inverse Gaussian model [3] and Kou's Jump-Diffusion model [34].

1.2 Volatility and Option Pricing

Assumptions on the second moment or variance of the stock price dynamics plays the most critical role in derivative pricing. This is because under the no-arbitrage assumption, the drift of the stock price process must equal the risk free rate under a change of measure. Thus, fluctuations in stock price volatility have the highest effect on the prices of derivatives. It is no surprise, therefore, that a need was felt in the markets to hedge volatility exposure. This led to the development of products like variance swaps, options on variance and volatility, and to some extent volatility swaps. See Javaheri [33] for a discussion on volatility hedging strategies.

However, pricing derivatives on volatility and the underlying index simultaneously is non-trivial. Any model for pricing volatility derivatives has to be consistent with the

underlying stock price process to avoid arbitrage. At the same time, the model has to capture features of volatility dynamics observed in the market. One such feature is the leverage effect. This is based on the observation that volatility increases as the stock prices go down and vice-versa. The leverage effect has been studied extensively in the financial literature. See Matacz & Potters [42], Yu [53] and Bollerslev, Litvinova & Tauchen [9] for more details and references. Finally, the model has to be parsimonious enough to allow for accurate and efficient computation.

Stochastic volatility models usually assume a negative correlation between the volatility and stock innovations. However, such models don't model the leverage effect since they don't have an explicit dependence on the level of the stock price. Some of these models also assume that the underlying stock price process has no jumps. This leads to underestimation of the prices of options of short maturity.

We believe that a reasonable model which captures the leverage effect should be able to capture prices of volatility derivatives in a one-dimensional framework. However, whether there is any need to include stochastic volatility as a hidden Markov process is a more profound question, which we will discuss in the section related to further research.

We propose a pure jump model which satisfies all our requirements to a significant extent. The dynamics of our model are governed by a pure jump Lévy process which is scaled by a function dependent on the underlying stock price. This scaling function captures the leverage effect. It also allows us to stay within a one-dimensional Markovian world since instantaneous volatility is modeled as a deterministic function of underlying stock price. This puts our model within the class of parametric pure

jump local volatility models. Local volatility models aim to calibrate option surfaces using a one-dimensional Markov model where the volatility is modeled as a function of the stock price and time. This approach was first used by Derman & Kani (see [21] and [22]), and Dupire [23]. Carr, Geman, Madan &Yor [14] later applied this technique to pure jump models. We will show that our model allows us to simultaneously and consistently price options on the stock and its volatility, for a given maturity.

1.3 VIX Index and Volatility Derivatives

The market for volatility derivatives had been over the counter (OTC) for a long time. Sufficient demand for volatility products has moved them into the mainstream of derivative products. Some of these volatility derivatives have even started trading in standardized form over the exchanges. One such exchange-traded volatility product is the VIX index. The VIX index tracks the expected one-month risk neutral volatility of the S&P500 (SPX) index in the market. In 2004, VIX futures started trading on the Chicago Board Options Exchange (CBOE); and in 2006, VIX options started trading on the CBOE options exchange. The development of this market has led to a demand for better models to calibrate VIX and SPX options simultaneously. We show that Lévy processes, which have been successful in calibrating to SPX options, are not suitable for pricing VIX options. We generalize the Lévy model by introducing space dependence in the pure jump framework. Our aim is to use these models for pricing options on VIX and SPX and then test them on market data.

1.3.1 Definition of the VIX Index

We start with the definition of the VIX index as defined by CBOE. We then generalize the definition to be consistent with a continuous time process. The CBOE defines the VIX index at time T as the market expectation of the average volatility over the next one month, that is volatility between T and $T+h$, where $h = 1/12$ (one month, measured in years). By market convention, the volatility is defined as the average quadratic variation over a one month period under the risk neutral measure . Let $\tilde{h}$ be the number of days between T and $T+h$. The VIX index at time T, V_T is defined as

$$V_T \quad := \sqrt{\frac{365}{\tilde{h}}} \sqrt{E_T \left[\sum_{t=\tilde{T}+1}^{\tilde{T}+h} x_t^2 \right]}, \tag{1.2}$$

$$x_t \quad := \ln \left(S_t / S_{t-1} \right). \tag{1.3}$$

Here $\tilde{T}$ is the number of days in T. The VIX index is quoted in annualized percent terms. Note that the square-root is outside the expectations since it is the expected variance that is backed out from option prices, and the volatility is reported as the square-root of that number. The options with one month maturity on the SPX index are used for calculating the VIX index. (see [56] for the details of the methodology).

As an example, if the VIX index is quoted as 30%, it means that the one-month volatility implied by option prices is approximately $30\%/\sqrt{12} = 8.66\%$. The one month variance backed out from option prices is $.0866^2 = 7.55\%$.

We note that the VIX index is a discrete time approximation of the quadratic

variation of the log-stock process $\ln S_t$, since it tracks the increments in the return process, x_t, once per day. We can generalize the definition of VIX above to measure the expected quadratic variation over any arbitrary window of time h (not necessarily 1/12), with any arbitrary frequency (not just once per day). Let h be a window of time, define Δt such that $1/\Delta t$ is the sampling frequency. Then the h-period VIX index at time T is defined as the T-conditional expected volatility for a period h

$$\begin{aligned} V_T &: = \sqrt{\frac{365}{\tilde{h}}} \sqrt{E_T \left[\sum_{t=\tilde{T}+1}^{\tilde{T}+\tilde{h}} x_t^2 \right]}, \text{ where} \\ x_t &: = \ln \left(S_t / S_{t-\Delta t} \right). \end{aligned} \tag{1.4}$$

Here $\tilde{h} := h/\Delta t$ and $\tilde{T} := T/\Delta t$ are the number of Δt-intervals in h and T respectively. This definition is consistent with a continuous time process in the sense that if we let $\Delta t \to 0$, the VIX index will give us the expected quadratic variation of a continuous price process, and not just its approximation. However, we will continue to assume that $\Delta t = 1$ day for the remaining part of our thesis.

1.3.2 Motivation Through The Variance Swap Arbitrage

A Variance Swap (VS) is a contract that pays the average realized variance over a period of time in exchange for a fixed coupon $\tilde{c}$. The payoff is defined as

$$VS\ payoff = \sum_{t=1}^{t=\tilde{T}} \left(\frac{x_t^2}{\tilde{T}} 365 - \tilde{c}^2 \right) \tag{1.5}$$

Here x_t is the same as in (1.2) and $\tilde{T}$ is the maturity of the swap measured in days. A variance swap contract can be replicated by options on the VIX index using the methodology of Carr & Madan [16]. It can also be replicated with options on SPX (see Carr & Madan [11]). However, the two methodologies give different prices for the variance swap contract in the market (a visible arbitrage!). This can only be avoided by using a model consistent with both SPX and the VIX option surfaces.

1.3.3 Derivatives on VIX

Most derivatives traded on VIX are quoted on its square-root. The most common ones are calls and puts. A call or a put option on the square-root of VIX with a strike price K and maturity T has a payout equal to $(V_T - K)^+$ or $(K - V_T)^+$, respectively. Note that the payoff depends only on the risk neutral expectations of quadratic variance and not on the realized quadratic variance. This is because the T-conditional expectation of the quadratic variation is known at T, as this expectation can be backed out of option prices on SPX. This means that the VIX option payoff is completely determined at T. The realized variance between T and $T + h$ does not contribute to the payoff.

1.3.4 Approximation of VIX

We observe that

$$\begin{aligned} e^x &= 1 + x + \frac{x^2}{2} + o(x^3), \\ \sum_{t=\tilde{T}+1}^{\tilde{T}+\tilde{h}} x_t^2 &\approx 2 \sum_{t=\tilde{T}+1}^{\tilde{T}+\tilde{h}} (e^{x_t} - 1) - 2 \sum_{t=\tilde{T}+1}^{\tilde{T}+\tilde{h}} x_t \\ \sum_{t=\tilde{T}+1}^{\tilde{T}+\tilde{h}} x_t^2 &\approx 2 \sum_{t=\tilde{T}+1}^{\tilde{T}+\tilde{h}} \left(\frac{S_t}{S_{t-1}} - 1 \right) - 2 \ln(S_{\tilde{T}+h}) + 2 \ln(S_{\tilde{T}}) \end{aligned} \tag{1.6}$$

We note that the error induced by truncation of the Taylor series is insignificant. To put this in perspective, daily changes of stock price are of the order of 1% of the stock price. Thus, terms of order x^3 are in the order of 0.0001% per day or about $30 \times 10^{-6} \approx 0.001\%$ for the one month period. This error will converge to *zero* as $\Delta t \to 0$ in (1.4), as the magnitude of the returns will also approach *zero* as $\Delta t \to 0$.

If the risk-free rate r is assumed to be constant, it is clear that

$$\begin{aligned} 2 \sum_{t=\tilde{T}+1}^{\tilde{T}+\tilde{h}} E_T \left[S_t / S_{t-1} - 1 \right] &= 2 \sum_{t=\tilde{T}+1}^{\tilde{T}+\tilde{h}} E_T \left[E_{t-1} \left[S_t / S_{t-1} - 1 \right] \right] \\ &= 2 \sum_{t=\tilde{T}+1}^{\tilde{T}+\tilde{h}} E_T \left[e^{r/365} - 1 \right] \\ &= 2h \left(e^{r/365} - 1 \right). \end{aligned} \tag{1.7}$$

Thus, the price, $c(r, h)$, of this cashflow at T is:

$$c(r, h) := 2h \left(e^{r/365} - 1 \right).$$

Taking T-conditional expectations, $E_T[\cdot]$, on both sides of (1.6) yields:

$$V_T \approx c(r,h) - 2E_T[\ln(S_{T+h})] + 2\ln(S_T). \tag{1.8}$$

We will rely on equation (1.8) heavily for pricing options on VIX. Most models for pricing volatility derivatives use the approach by Carr and Madan [16]. They first price options on variance using the log contract, which itself is priced as a portfolio of Out of The Money (OTM) calls and puts on the underlying stock. OTM call options are defined as options with strike price greater than the current stock price. OTM puts are options with strike price less than the current stock price. The volatility derivatives are then priced as a portfolio of options on variance.

1.3.5 Stationary processes and VIX modeling

From (1.8), we see that

$$V_T \approx c(r,h) - 2E_T[X_{T+h}] + 2X_T. \tag{1.9}$$

If X_t follows a stationary process, then the innovation $X_{T+h} - X_T$ is independent of the time T. Thus, we have that

$$\begin{aligned} V_T &\approx c(r,h) - 2E_T[X_{T+h} - X_T] \\ V_T &\approx c(r,h) - 2E[X_h] \\ V_T &\approx \text{constant}. \end{aligned} \tag{1.10}$$

A result more precise than (1.10) above can be arrived at by noting that the quadratic variation of a Lévy process is also a Lévy process (see [17]) and hence is a stationary process. The reason for keeping the above equation is that it gives a better overview of different approaches that can be applied to model the VIX index. Essentially, all approaches will model the increment at T, $E_T\left[X_{T+h} - X_T\right]$. In our approach we assume that $E_T\left[X_{T+h} - X_T\right] = f(X_T)$. Models based on stochastic volatility assume that $E_T\left[X_{T+h} - X_T\right] = f(v)$, where v is a hidden Markov process. The more general approach would make

$$E_T\left[X_{T+h} - X_T\right] = f(t, X_T, v, Y_T), \tag{1.11}$$

which incorporates the effects of time decay, stock level, stochastic volatility as well as other hidden or observed processes, captured in Y_T.

The above result in (1.10) holds irrespective of the level of X_T as there is no dependence of the increments on X_T due to stationarity. This shows that stationary processes are unable to capture any uncertainty in VIX. Such processes can only value a VIX option as its intrinsic value without attributing any time value to it. We would ideally need a model that maintains dependency of $E_T\left[X_{T+h} - X_T\right]$ on (T, X_T). Our model takes a step in this direction by modeling dependence on X_T. We leave out an explicit dependence on T for reasons we will explain later in this dissertation. Our model proposes space-dependency in a pure jump processes framework.

1.3.6 Leverage Effect and VIX modeling

Since our aim is to provide a model which can price volatility derivatives, we want to be able to capture the commonly observed features of volatility and stock returns. It is a common observation that volatility rises as stock prices fall and vice-versa. One possible reason for this effect is the 'fear-factor' - increase in uncertainly and fear if stock prices fall. This relationship between volatility and stock-level is also known as the leverage-effect and has been widely studied in the financial literature. We capture this relationship in our model through the (innovatively named!) 'leverage function' $a(x)$, where x is the log-stock level. We model the leverage function as a bounded quadratic function in the log-stock variable. We define it formally in equation (3.5) below. However, as we will see from the estimations, only the negative arm of the parabola is required to capture the leverage function.

Chapter 2

Lévy Processes

All Lévy processes are processes with infinitely divisible distributions. These processes have homogenous and independent increments. A Lévy process $Z(t)$ is best characterized by the Lévy-Khintchine formula which describes the characteristic function for the marginal distributions as:

$$E(\exp^{iuZ(t)}) = \exp(iu\mu t - \frac{1}{2}\sigma^2 u^2 t + t\int_{-\infty}^{\infty}(e^{iuz} - 1 - iuz1_{\{|z|\leq 1\}})k(z)dz). \qquad (2.1)$$

where μ is the drift coefficient, σ is the diffusion coefficient, $k(z)$ gives the Lévy density (which we will define and discuss in greater detail below) and $1_{\{.\}}$ is the indicator function. We note that if $k(z) \equiv 0$, we get a diffusion process with mean μ and variance σ^2. Lévy processes can be seen as a generalization of the diffusion process. On the other hand if the the diffusion coefficient σ is zero, the resulting process is a pure jump Lévy process. The Lévy density $k(z)$ is assumed to have finite

quadratic variation, which is equivalent to the condition that

$$\int_{-\infty}^{\infty}(|z|^2 \wedge 1)k(z)dz < \infty, \tag{2.2}$$

where $\wedge$ is the minimum operator. If the Lévy density satisfies the following condition:

$$\int_{-\infty}^{\infty} z^2 k(z)dz < \infty, \tag{2.3}$$

then we can rewrite the Lévy-Khintchine formula as

$$E(\exp^{iuZ(t)}) = \exp(iu\mu t - \frac{1}{2}\sigma^2 u^2 t + t\int_{-\infty}^{\infty}(e^{iuz} - 1 - iuz)k(z)dz). \tag{2.4}$$

If the Lévy process has finite variation whereby $\int_{-\infty}^{\infty}(|z| \wedge 1)k(z)dz < \infty$, the above formula can be further simplified to

$$E(\exp^{iuZ(t)}) = \exp(iu\mu t - \frac{1}{2}\sigma^2 t + t\int_{-\infty}^{\infty}(e^{iuz} - 1)k(z)dz). \tag{2.5}$$

For further details, see [7] and [50]. Let $\varepsilon > 0$. A pure jump process with finite variation can always be approximated by a compound Poisson process with the arrival rate

$$\lambda = \int_{|z|>\varepsilon} k(z)dz < \infty \tag{2.6}$$

and the jump density, conditional on arrival, is given by

$$g(z) = \frac{k(z)1_{\{|z|>\varepsilon\}}}{\lambda} \tag{2.7}$$

The convergence in distribution occurs as $\varepsilon \to 0$. When $\int_{-\infty}^{\infty} k(z)dz = \infty$, we say that the Lévy process has infinite activity. This means that an infinite number of jumps occur in any arbitrarily small interval of time. Most pure jump Lévy processes used in financial modeling are infinite activity processes. We now describe two of the pure jump Lévy processes used for modeling stock returns. We will start with a brief description of the Variance Gamma process. We then describe the CGMY process and show the relation between the VG and the CGMY processes. We will construct our space scaled process from the CGMY process.

2.1 Variance Gamma (VG) Process

The first model using symmetric pure jumps to appear in the literature was the symmetric Variance Gamma (VG) model by Madan and Seneta [39] and Madan and Milne [38]. It is a process of infinite activity and finite variation. Madan, Carr and Chang [13] later generalized the VG process to one with asymmetric jumps. They use numerical estimations over options and daily returns data to show that this process is better suited to describing stock price dynamics than a diffusion based model with no jumps. They showed that this model can be viewed as a time-changed Brownian motion evaluated at Gamma time. They also show that the Lévy density of the VG process is given by

$$k(z) = \begin{cases} C\frac{\exp(Gz)}{|z|} \text{ for } z < 0 \\ C\frac{\exp(-Mz)}{|z|} \text{ for } z > 0 \end{cases}.$$

2.2 CGMY Process

The CGMY Process was introduced by Carr, Geman, Madan and Yor [10]. It is an extension of the VG process with an extra parameter Y . This parameter controls the activity, variation and monotonicity properties of the pure jump component. The Lévy measure for a CGMY process is given by

$$v(x) = \begin{cases} C\frac{\exp(-G|z|)}{|z|^{1+Y}} \text{ for } x < 0 \\ C\frac{\exp(-M|z|)}{|z|^{1+Y}} \text{ for } x > 0 \end{cases} .$$

We provide the result for the characteristic function of the CGMY process.

Theorem 1 *The characteristic function of the CGMY process is given by*

$$\phi_{CGMY}(u,t) = \begin{cases} \exp\left(Ct\Gamma(-Y)(\left((M-iu)^Y - M^Y\right)\right) \times \\ \exp\left(Ct\Gamma(-Y)\left((G+iu)^Y - G^Y\right)\right) \end{cases} .$$

Proof. For the proof, see Carr, Geman, Madan & Yor [10]. ■

2.3 Numerical Methods in Derivative Pricing

The Black-Scholes process has closed form solutions for European Call and Put options as well as some barrier options. However for more general processes, one requires numerical methods to price options. There are three main numerical approaches used in finance: numerical partial (integro) differential equations (PDEs or PIDEs), Monte Carlo simulations of the stochastic differential equation and Fourier methods. Processes based on diffusion equations are generally easy to implement numerically

using any of these methods. This is because the numerical solutions to PDEs generated by these processes are based on solving linear systems with sparse matrices. In case of Monte Carlo simulations, the underlying process can be generated by simulating standard normal random variables which is also easy and efficient to implement. Further, one has access to closed form solutions of the characteristic function of the stock price process which allows the use of Fourier methods.

The choice of numerical implementation is based on three main issues: the complexity of the underlying derivative contract payoff, the speed restrictions on computation (i.e. live pricing and calibration requirements) and the accuracy required. Let us analyze these methods in the context of our problem.

2.3.1 Simulation Methods

Simulation based methods rely on being able to simulate the stock price process through its stochastic differential equation. The main advantage of simulation based methods is that they are very versatile in pricing complex payoffs. However, since one may require large number of simulation paths for convergence, one has to compromise on speed or accuracy in the process. Simulation methods become prohibitively expensive when one needs to calibrate the underlying model to market prices as one would then need to run the simulation inside a parameter optimizing iterative program to minimize the error between model and market prices. Since this is precisely what we aim to do with our model, we will have to rule out using a simulation scheme.

2.3.2 Fourier Methods

The second method of pricing derivatives is through the characteristic function (Fourier transform) of the underlying stock process. Madan and Carr [12] invented the methodology to obtain option prices efficiently through the characteristic function of the marginal stock price distributions using Fast Fourier Transforms (FFT). This method is robust and efficient, but only works when the characteristic function is known in closed form. In a pure jump process setting, the characteristic function is usually computable when the increments in the stock price process do not dependent on the level of the stock price, that is, there is no space dependence in the stock price process. However, in our model, we do have space dependence through the leverage function, thus don't have a closed form formula for the characteristic function. This comprehensively rules out using the Fourier methods.

2.3.3 Numerical Partial (Integro) Differential Equations

The third method to price derivatives is through numerical PDEs or PIDEs. This method used to be computationally intensive when the underlying process is a pure jump Lévy process. However, recent advances in finite element method using wavelet compression technology devised by Matache, von Petersdorff and Schwab [41] , and von Petersdorff and Schwab [47] have greatly increased the efficiency of this methodology and it compares well with FFT methods. This methodology is also preferable in cases where the characteristic function is not available in closed form. This is usually the case whenever the transition densities of the stock price process depend on the

level of the stock. This is the situation we will face with our proposed model.

We use Finite Element Method for solving the PIDE of the pure jump space scaled process. Our aim in this dissertation is to show the advantages of such a model. We do not yet focus on the efficiency of our numerical solver. We do however highlight schemes which can be used in making our solver more efficient so it can be used for real-time calibration and pricing.

2.4 Stock Price Dynamics under Lévy Processes

Our aim is to describe the stock price dynamics under our space scaled Lévy process. Since our model is a generalization of Lévy processes, we start by describing the stock price process under Lévy processes. For this we follow the derivation of the stock price dynamics in Cont and Tankov [18] and Protter [49]. We assume that the stock price follows an exponential Lévy process under the risk neutral measure Q given by

$$S_t = S_0 e^{rt+Y_t+\omega t}. \tag{2.8}$$

Here Y_t is a pure jump Lévy process. We need the convexity correction term ωt to ensure that the stock has a mean growth rate of r, i.e.

$$\begin{aligned} E^Q[S_t] &= S_0 e^{rt}, \quad \text{or} \\ \omega &= t^{-1} \ln(1/E^Q[e^{Y_t}]). \end{aligned}$$

The dynamics of the stock price process is then given by (see [18] and [19])

$$dS_t = (r+\omega)S_{t-}dt + S_{t-}\int_{-\infty}^{\infty}(e^z - 1 - z)\, J_Y(dz, dt).$$

where $J_Y(dz, dt)$ is the counting measure of random jumps of size between z and $z + dz$ in the time interval dt. For Lévy processes, the compensator of this measure is $k(z)dzdt$ where $k(z)$ is the Lévy density. We define

$$\tilde{J}_Y(dz, dt) := J_Y(dz, dt) - k(z)dzdt \tag{2.9}$$

to be the compensated pure jump process. We can then rewrite the above equation as

$$\begin{aligned} dS_t &= (r+\omega)S_{t-}dt + S_{t-}\int_{-\infty}^{\infty}(e^z - 1 - z)\, \tilde{J}_Y(dz, dt) \\ &\quad + \int_{-\infty}^{\infty}(e^z - 1 - z)\, k(z)dzdt. \end{aligned} \tag{2.10}$$

Since we want this process to grow at the rate r, we impose the drift condition

$$\omega + \int_{-\infty}^{\infty}(e^z - 1 - z)\, k(z)dz = 0. \tag{2.11}$$

Let $f(t, S_t)$ be the price of a contingent claim on S_T with the payoff at time T given by $\tilde{h}(S_T)$. Then by an extension of Ito's lemma for Lévy processes (see Cont and

Voltchkova [19]), the dynamics of $f(t, S_t)$ are given by

$$\begin{aligned} df(t,S_t) &= \frac{\partial f(t,S_{t-})}{\partial t}dt + \int_{-\infty}^{\infty}(f(t,S_{t-}e^z) - f(t,S_{t-}))dJ_Y(dz,dt) \\ &= \frac{\partial f(t,S_{t-})}{\partial t}dt + (r+\omega)S_{t-}\frac{\partial f(t,S_{t-})}{\partial S}dt \\ &\quad + \int_{-\infty}^{\infty}(f(t,S_{t-}e^z) - f(t,S_{t-}) - zS_{t-}\frac{\partial f(t,S_{t-})}{\partial S})d\tilde{J}_Y(dz,dt) \\ &\quad + \int_{-\infty}^{\infty}(f(t,S_{t-}e^z) - f(t,S_{t-}) - zS_{t-}f(t,S_{t-}))k(z)dzdt. \end{aligned}$$

We can rewrite the above equation as

$$\begin{aligned} df(t,S_{t-}) &= \mu(t,S_{t-})dt + dM_t, \text{ where} \\ dM_t &= \int_{-\infty}^{\infty}(f(t,S_{t-}e^z) - f(t,S_{t-}) - zS_{t-}\frac{\partial f(t,S_{t-})}{\partial S})d\tilde{J}_Y(dz,dt), \text{ and} \\ \mu(t,S_{t-}) &= \frac{\partial f(t,S_{t-})}{\partial t} + (r+\omega)S_{t-}\frac{\partial f(t,S_{t-})}{\partial S} \\ &\quad + \int_{-\infty}^{\infty}(f(t,S_{t-}e^z) - f(t,S_{t-}) - S_{t-}zf(t,S_{t-}))k(z)dz. \end{aligned}$$

By the above condition on ω,

$$\begin{aligned} \mu(t,S_{t-}) &= \frac{\partial f(t,S_{t-})}{\partial t} + rS_{t-}\frac{\partial f(t,S_{t-})}{\partial S} \\ &\quad + \int_{-\infty}^{\infty}(f(t,S_{t-}e^z) - f(t,S_{t-}) - S_{t-}\frac{\partial f(t,S_{t-})}{\partial S}(e^z-1))k(z)dz. \end{aligned}$$

Since asset prices grow at the mean rate of r under the risk neutral measure,

equating $\mu(t, S_t)$ to $rf(t, S_t)$ gives the PIDE for Lévy Processes

$$\frac{\partial f(t,S)}{\partial t} + rS\frac{f(t,S)}{\partial S} +$$
$$\int_{-\infty}^{\infty} (f(t, Se^z) - f(t,S) - Sf'(t,S)\,(e^z - 1))k(z)dz - rf(t,S) = 0, \tag{2.12}$$

$$f(T, S_T) = \tilde{h}(S_T). \tag{2.13}$$

2.5 Stock Price Process with Dividends

When the dividend rate is positive, the stock price is given by

$$S_t = S_0 e^{(r-q)t + Y_t + \omega t}. \tag{2.14}$$

This gives us the dynamics

$$\begin{aligned} dS_t &= (r - q + \omega)S_{t-}dt + \int_{-\infty}^{\infty} (e^z - 1 - z)\,\tilde{J}_Y(dz, dt) \\ &\quad + \int_{-\infty}^{\infty} (e^z - 1 - z)\,k(z)dzdt. \end{aligned}$$

Since the martingale condition implies that the expected future stock price (along with the accumulated dividends), i.e. $S_t e^{qt}$ discounted by the risk free rate, is the

spot price, applying this at time zero we get

$$\begin{aligned} S_0 &= e^{-rt} E^Q \left[S_0 e^{(r-q+\omega)t+Y_t} e^{qt} \right], \text{ or} \\ \omega &= t^{-1} \ln(1/E^Q[e^{Y_t}]). \end{aligned}$$

This implies the same drift condition as above

$$\omega + \int_{-\infty}^{\infty} (e^z - 1 - z)\, k(z) dz = 0.$$

Similarly, the dynamics $f(t, S_t)$ of a contingent claim paying $f(T, S_T) = h(S_T)$ at time T, are given by

$$\begin{aligned} df(t, S_{t-}) &= \mu(t, S_{t-})dt + dM_t, \text{ where} \\ dM_t &= \int_{-\infty}^{\infty} (f(t, S_{t-}e^z) - f(t, S_{t-}) - zS_{t-}\frac{\partial f(t, S_{t-})}{\partial S}) d\tilde{J}_Y(dz, dt), \text{ and} \\ \mu(t, S_{t-}) &= \frac{\partial f(t, S_{t-})}{\partial t} + (r - q + \omega) S_{t-} \frac{\partial f(t, S_{t-})}{\partial S} \\ &\quad + \int_{-\infty}^{\infty} (f(t, S_{t-}e^z) - f(t, S_{t-}) - S_{t-} z \frac{\partial f(t, S_{t-})}{\partial S}) k(z) dz. \end{aligned}$$

Again the risk neutral growth rate of r implies that $\mu(t, S_{t-}) = r$, giving us the PIDE

$$\begin{aligned} &\frac{\partial f(t, S)}{\partial t} + (r - q) S \frac{\partial f(t, S)}{\partial S} \\ &+ \int_{-\infty}^{\infty} (f(t, Se^z) - f(t, S) - S \frac{\partial f(t, S)}{\partial S} (e^z - 1)) k(z) dz - r f(t, S) = 0. \end{aligned} \tag{2.15}$$

$$f(T, S_T) = h(S_T).$$

We see that $f(t, S_t) = S_t e^{qt}$ satisfies the equation above since

$$LHS = qS_t + (r-q)S_t + \int_{-\infty}^{\infty} (S_t e^z - S_t - S(e^z - 1))k(z)dz - rS = 0.$$

Also the Bond Price $B(t,T) = e^{-r(T-t)}$ satisfies the PIDE since

$$LHS = rB(t,T) + \int_{-\infty}^{\infty} (B(t,T) - B(t,T) - 0)k(z)dz - rB(t,T) = 0.$$

Let $x = \ln(S)$. Also let $f(t,S) = g(t,x)$ and $\tilde{h}(S) = h(x)$. We would like to re-derive the equation (2.15) in terms of g and x. We note that $\frac{\partial g}{\partial t} = \frac{\partial f}{\partial t}$ and $\frac{\partial g}{\partial x} = \frac{\partial g}{\partial x}/S$. Using these in (2.15) gives

$$\frac{\partial g}{\partial t}(t,x) + (r-q)\frac{\partial g}{\partial x}(t,x) +$$
$$\int_{-\infty}^{\infty} (g(t,x+z) - g(t,x) - \frac{\partial g}{\partial x}(t,x)\,(e^z - 1))k(z)dz - rg(t,x) = 0. \tag{2.16}$$

$$g(t,x) = h(x) \tag{2.17}$$

Rewriting the price dynamics in terms of time to maturity $w(\tau, x) = g(T-t, x)$, we have the PIDE

$$\frac{\partial w}{\partial \tau}(\tau,x) - (r-q)\frac{\partial w}{\partial x}(\tau,x) + rw(\tau,x) \tag{2.18}$$
$$-\int_{-\infty}^{\infty} (w(\tau,x+z) - w(\tau,x) - \frac{\partial w}{\partial x}(\tau,x)\,(e^z - 1))k(z)dz = 0, \tag{2.19}$$

$$w(0,x) = h(x) \tag{2.20}$$

To simplify our notation, let us define the two operators A and $\hat{A}$ as

$$\begin{aligned}\hat{A}[w](\cdot) &: = -\int_{-\infty}^{\infty}(w(\tau,\cdot+z)-w(\tau,\cdot)-\frac{\partial w}{\partial x}(\tau,\cdot)\,(e^z-1))k(z)dz \text{ and}\\ A[w](\cdot) &: = \hat{A}[w](\tau,\cdot)-(r-q)\frac{\partial w}{\partial x}(\tau,\cdot)+rw(\tau,\cdot)\end{aligned}$$

2.6 PIDE under no drift condition

We follow the steps described in Matache, von Petersdorff and Schwab (see [41]) in setting up the variational formulation. We first describe the case when interest rate and dividend rate are both zero, i.e. $r = 0$ and $q = 0$. We note that in this case $A = \hat{A}$. For a pure jump process, the PIDE reduces to

$$\begin{aligned}\frac{\partial g}{\partial \tau}(\tau,x)+Ag(\tau,x)&=0, \qquad (2.21)\\ Ag(\tau,\cdot) := -\int_{-\infty}^{\infty}\left(g(\tau,\cdot+z)-g(\tau,\cdot)-\frac{\partial g}{\partial \tau}(\tau,\cdot)(e^z-1)\right)k(z)dz;&\\ g(0,x)=h(x).&\end{aligned}$$

We transform the PIDE to solve for the excess value function $u(\tau,x) := g(\tau,x)-h(x)$. This transformation gives us a PIDE with a homogenous initial condition

$$\begin{aligned}\frac{\partial u}{\partial \tau}(\tau,x)+Au(\tau,x) &= -Ah(x),\\ h(x) &= 0.\end{aligned}$$

2.6.1 Variational Formulation

While the call option payoff in log-stock variable grows exponentially as $x \to \infty$, Matache, von Petersdorff and Schwab [41] show that the transformed value function $u(\tau, x)$ decays exponentially as $x \to \infty$. Hence, we assume that the solution $u(\tau, x)$ as a function of x, belongs to $L^2(\mathbb{R})$. We consider a test function $v \in C_0^\infty(\mathbb{R})$, the space of all infinitely differentiable functions with bounded support. Define the inner product

$$(u, v) = \int_{-\infty}^{\infty} u(x)v(x)dx. \tag{2.22}$$

Multiplying both sides of (2.18) with $v(x)$ and integrating over $\mathbb{R}$

$$\begin{aligned} &(\frac{\partial u}{\partial \tau}(x), v(x)) + (Au(x), v(x)) = -(Ah(x), v(x)). \text{ Or} \\ &\partial(u, v)/\partial\tau + \tilde{a}(u, v) = -(Ah, v), \text{ where} \\ &\tilde{a}(u, v) = (Au, v). \end{aligned} \tag{2.23}$$

This gives us the weak form of the PIDE under a driftless stock price process.

2.7 PIDE under positive interest and dividend rate assumption

When interest rates are positive, the asymptote for the solution $u(\tau, x)$ is no longer $h(x)$ but $h(x + (r - q)\tau)e^{-r\tau}$. We define the excess value function as $u(x) = w(x) - h(x + (r - q)\tau)e^{-r\tau}$. We transform the PIDE to solve for the excess value function to

get

$$\begin{aligned} u(x) &= w(x) - h(x + (r-q)\tau)e^{-r\tau} \qquad (2.24) \\ \frac{\partial u}{\partial \tau}(x) + Au(x) &= -\hat{A}_x h(x + r\tau)e^{-r\tau}, \\ \text{Initial Condition} &: \quad h(x) = 0. \end{aligned}$$

2.7.1 Variational Formulation

Proceeding as above by multiplying a test function $v \in C_0^\infty(\mathbb{R})$ on both sides and integrating, we get the 'weak form' of the PIDE

$$(\frac{\partial u}{\partial \tau}(\cdot), v(\cdot)) + (Au(\cdot), v(\cdot)) = -(\hat{A}h(\cdot + r\tau)e^{-r\tau}, v(\cdot)). \qquad (2.25)$$

$$\partial(u,v)/\partial\tau + \tilde{a}(u,v) = (\tilde{f}_\tau, v), \text{ where}$$

$$\tilde{a}(u,v) = (Au(\cdot), v(\cdot))$$

$$(\tilde{f}_\tau, v) = -(\hat{A}h(\cdot + r\tau)e^{-r\tau}, v(\cdot))$$

For Lévy processes, without loss of generality one can transform the case $r > 0$ to $r = 0$ with the transformation $\tilde{u}(\tau, x) = e^{r\tau}u(\tau, x + (r-q)\tau)$. See Matache, von Petersdorff and Schwab [41] for more details. We can therefore restrict our attention to the case with zero interest rate for Lévy processes. We will take up the case of positive interest rates where we deal with the space-scaled Lévy processes in the next chapter.

2.7.2 Localization of the PIDE

We restrict the PIDE to $J \times \Omega_R$, where $\Omega_R = [-R, R] \subset \mathbb{R}$. Let $A_R[\cdot]$ denote the restriction of the operator $A[\cdot]$ to Ω_R and u_R denote the solution of the PIDE restricted to Ω_R

$$(\frac{\partial u_R}{\partial \tau}, v) + (A_R u_R, v(x)) = -(Ah, v)|_{\Omega_R}. \text{ Or}$$

$$\partial(u_R, v)/\partial t + a_R(u_R, v) = (f, v), \text{ where}$$

$$u_R(x) = \begin{cases} u(x), \ x \in \Omega_R \\ \\ 0, \ x \in \partial\Omega_R, \end{cases}$$

$$a_R(u_R, v) = (A_R u_R, v), \quad \text{and}$$

$$(f, v) = -(A_R h, v).$$

If $U(t, x)$ is the solution of the PIDE (2.18) and $U_R(t, x)$ is the restriction of the solution over the solution, it has been shown in [41] that for $\varepsilon_R = U(t, x) - U_R(t, x)$, there exists an $\alpha > 0$ and a $C = C(T)$ such that for all $R > 0$,

$$\|\varepsilon_R(\tau, \cdot)\|_{L^2(\Omega_R)} + \int_0^\tau \|\varepsilon_R(s, \cdot)\|_{H^1(\Omega_R)} \, ds < Ce^{-\alpha R}$$

Thus the localization error is decreases exponentially as one increases the diameter of the localized space.

2.8 Overview of Finite Element Method for solving PIDEs

2.8.1 Discretization of the PIDE

We assume $r = 0$ since the case $r > 0$ can be transformed to $r = 0$ as described above. Let H_N be the space of all continuous and piecewise linear functions on a grid x_j, $j = 0, 1, ..., N+1$, with compact support. Let $\{\phi_i\}_{i=1}^{N}$ be a set of 'hat functions' which span H_N. We look for a solution to the PIDE in this subspace. The hat function ϕ_j has support in $[x_{j-1}, x_{j+1}]$ and attains the value 1 at x_j

$$\begin{aligned} \phi_j(x) &= \begin{cases} \frac{(x-x_{j-1})}{h_j} & \text{for } x \in [x_{j-1}, x_j] \\ \frac{(x_{j+1}-x)}{h_{j+1}} & \text{for } x \in [x_j, x_{j+1}] \end{cases} \\ \phi_j'(x) &= \begin{cases} \frac{1}{h_j} & \text{for } x \in [x_{j-1}, x_j] \\ \frac{-1}{h_{j+1}} & \text{for } x \in [x_j, x_{j+1}] \end{cases} \end{aligned} \tag{2.26}$$

Let m denote the time-step index: $m = 0, 1, ..., M$; $\Delta t = T/M$. We look for the approximate solution $u^m(x)$ at time $t = m\Delta t$

$$u^m(x) = \sum_{i=1}^{N} u_i^m \phi_i(x), \tag{2.27}$$

If we let $v = \phi_i, i = 1, ..., N$ and substitute (2.27) in equation (2.23) we get

$$\Delta t^{-1} \sum_{j=1}^{N} u_j^m(\phi_j, \phi_i) - \Delta t^{-1} \sum_{j=1}^{N} u_j^{m-1}(\phi_j, \phi_i) \tag{2.28}$$
$$+ \sum_{j=1}^{N} \left(\theta u_j^m + (1-\theta) u_j^{m-1}\right) \tilde{a}(\phi_j, \phi_i) = (f_t, \phi_i) \qquad \text{for } i = 1, ..., N.$$

Here $\theta \in [0, 1]$. The value of θ denotes the time-stepping scheme. We get the backward Euler for $\theta = 1$, the Crank-Nicholson for $\theta = .5$ and the forward Euler method for $\theta = 0$. For more details, please refer to [54].

2.8.2 Matrix form of the PIDE

The above equation (2.28) can be rewritten in a matrix form as

$$\Delta t^{-1}(Mu^m - Mu^{m-1}) + \theta A u^m + (1-\theta) A u^{m-1} = F, \tag{2.29}$$

$$u^m = ((M + \Delta t \theta A))^{-1} \left(Mu^{m-1} + \Delta t F - \Delta t (1-\theta) A u^{m-1}\right)$$

$$M_{ij} := (\phi_j, \phi_i);$$

$$A_{ij} := \tilde{a}(\phi_j, \phi_i);$$

$$F^i := -(Ah, \phi_i).$$

We call M the mass matrix, A the stiffness matrix and F the RHS vector.

Efficient schemes for solving the PIDE above have been constructed in Matache, von Petersdorff and Schwab in [41]. These schemes rely on using a wavelet basis instead of the basis of hat functions. This basis allows for compression of the stiffness

matrix to the order of $N \ln N$ non-zero entries as compared to N^2 entries on a stiffness matrix based on hat functions. It also has the advantage that the stiffness matrix has a condition number which does not depend on the step size of the space discretization. This allows for the use of iterative methods for the solution without compromising on numerical accuracy or efficiency. This method is the method of choice when one needs large degrees of freedom (greater than 100) in space. We find that for our purpose, around 28degrees of freedom were sufficient. Hence this did not necessitate the use of wavelet compression. This is however a powerful avenue to be explored for computations involving greater accuracy, like the option Greeks.

2.8.3 Existence of a Solution

We give the theoretical setting for the existence of the weak solutions of the parabolic problem (2.23). We formulate the result for $r = 0$ and $q = 0$. We give the justification why the result holds even when $r > 0$ and $q > 0$ as well. Let $A : V \to V^*$ be an elliptical operator of order Y which maps a space V to its dual space V^*. We have the relation, known as the Gelfand triple, that

$$V \subset H \subset V^*,$$

with $V = \tilde{H}^{\frac{Y}{2}}(\Omega), H = L^2(\Omega)$ and $V^* = \tilde{H}^{\frac{-Y}{2}}(\Omega)$. Here $\tilde{H}^s$ is a Sobolev space of order s such that all functions in $\tilde{H}^s$ are *zero* on $\partial\Omega$. See Matache, von Petersdorff and Schwab [41] for more details on Sobolev spaces. Then under the assumptions of

continuity, defined as

$$|(Au, v)_{V^* \times V}| \leq C_0 \|u\|_V \|v\|_V, \quad \text{for all } u, v \in V, \text{ for some } C_0, \tag{2.30}$$

and coercivity, which is defined as

$$|(Au, u)| \geq C_1 \|u\|_V^2, \quad \text{for all } u \in V, \text{ for some } C_1, \tag{2.31}$$

a solution to the parabolic problem (2.23) exists. See von Petersdorff and Schwab [41] for the characterization of the solution. In the case where $r > 0$ and $q > 0$, one can use an exponential transformation $\tilde{u}{=}e^{-Ct}u$ to transform the parabolic equation into another equation which satisfies (2.30) and (2.31).

2.8.4 Error Estimates

Let $U(t, x)$ be the approximate solution and $u(t, x)$ be the true solution. For a parabolic equation with smooth initial conditions, it has been shown in Thomée [55], Theorem 1.5 that,

$$\|U^m - u(T, \cdot)\|_{L^2} \leq \begin{cases} C_1 (\Delta x)^2 + C_2 \Delta t & \text{for } \theta \neq \frac{1}{2} \\ C_1 (\Delta x)^2 + C_2 (\Delta t)^2 & \text{for } \theta = \frac{1}{2} \end{cases}. \tag{2.32}$$

Here In Theorem 5.4 of Schwab and von Petersdorff [47], it has been shown that for $\theta \neq \frac{1}{2}$ for smooth initial conditions that

$$\left(k \sum_{m=0}^{M} \|U^m - u(t_m, \cdot)\|_{H^s}^2 \right)^{1/2} \leq C_3 \left(\Delta x\right)^{2-s} + C_4 \Delta t. \tag{2.33}$$

This result is generalized for non-smooth initial data in Schwab and von Petersdorff [48].

Chapter 3

Space Scaled Lévy Processes

3.1 Introduction

We aim to introduce space dependence though scaling jumps of a Lévy process. It has been observed that when stock prices go down, volatility rises and vice versa. Our aim is to capture this dependence of volatility on the underlying stock. Since Lévy processes are stationary, their volatility is independent of the level of the stock price. At the same time, they exhibit other features like skewness and kurtosis which are desirable in our density. We propose a model which generalizes the Lévy process framework by introducing space dependence. The space dependence parameters allow for different levels of dependence and include the possibility of stationary and homogenous increments. We start with a Lévy process. We work with the CGMY model for the Lévy process because of its relative ease in computing numerical solutions. We call the resulting process CGMY Spaced-Scaled-Lévy Process (CGMYSSL). Let $X_t = \log(S_t)$, where the dynamics of S_t are given by (2.14). We now define the

process Y_t in (2.14). Let $\tilde{Y}_t$ be a Lévy process. We define the scaled-Lévy process by the relation

$$\Delta Y_t := a(X_{t-})\Delta\tilde{Y}_t, \tag{3.1}$$

where $a(x)$ is a leverage function. We assume that $0 < a(x) < \zeta$ for all x for some $\zeta > 0$. The boundedness of $a(x)$ is required to ensure that the stock price process has finite moments. Let z be the Lévy-jump size and $\tilde{z}$ denote the corresponding jump in the scaled process Y_t. Let $a(x)$ be the leverage function described above. Then

$$\tilde{z} = a(x)z \tag{3.2}$$

Let $k_{l\acute{e}vy}(z)$ denote the Lévy density of the Lévy process $\tilde{Y}_t$. We use it to derive the Lévy system density of the scaled-Lévy process Y_t:

$$k_{l\acute{e}vy}(z)dz = k_{l\acute{e}vyssl}\left(\frac{\tilde{z}}{a(x)}\right)\frac{d\tilde{z}}{a(x)}. \tag{3.3}$$

3.2 CGMY Space Scaled Process

We derive the Lévy-system density CGMY Space Scaled Volatility (CGMYSSL) process from the Lévy density of the CGMY process.

$$\begin{aligned} k_{cgmyssl}(z,x) &= k_{cgmy}\left(z/a(x)\right)/a(x) \\ &= \begin{cases} Ca(x)^Y \frac{\exp(-\frac{M}{a(x)}z)}{z^{1+Y}} & \text{for } z < 0 \\ Ca(x)^Y \frac{\exp(-\frac{G}{a(x)}|z|)}{|z|^{1+Y}} & \text{for } z > 0. \end{cases} \end{aligned} \tag{3.4}$$

We assume that the scaling function $a(x)$ is a capped-quadratic.

$$a(x) = \begin{cases} \min(\alpha + \beta(x-\xi)^2, \zeta) \\ \\ \zeta = \min(G, M) - \varepsilon, \end{cases} \tag{3.5}$$

$$\text{where } \varepsilon > 0, \text{ and } \alpha > 0, \ \beta \geq 0 => a(x) > 0.$$

The cap by ζ is due to the integrability requirement that $\int_{-\infty}^{\infty} e^z k(z,x)dz < \infty$. Note that $\beta = 0$ gives us a CGMY process with $\tilde{G} = G/\alpha$, $\tilde{M} = M/\alpha$ and $\tilde{C} = C\alpha^Y$. In addition, if we have $\alpha = 1$, we get back the original CGMY process.

3.2.1 Scaling function: some properties

Without loss of generality, we only consider $z > 0$. This is because the jump activity of both positive and negative jumps has the same functional form and our analysis for the effect of the scaling function on jump activity holds for negative jump as well, with the parameter M replaced by G. We note that

$$k_{cgmhssl}(z,x) = a(x)^Y k_{cgmy}\left(z; \frac{M}{a(x)}\right). \tag{3.6}$$

When $a(x) \approx 0$, the intensity of jumps decreases. Jump sizes also decay faster as $M/a(x)$ is large. When $a(x) > 1$, the jump intensity increases and so does the probability of large jumps due to smaller decay by $M/a(x)$. Thus $a(x)$ changes the behavior of the jump sizes based on the level of the log-stock.

3.3 PIDE for Space Scaled Processes

We derived the PIDE for the pure jump Lévy processes in (2.15) above. For a space-scaled process, the Lévy density $k(z)$ is replaced by the Lévy system density $k(z,x)dz$ of the space-scaled process to get the PIDE.

$$w_\tau(\tau,x) + Aw(\tau,x) = 0, \tag{3.7}$$

$$Aw(\tau,x) = -(r-q)w_x(\tau,x) + rw(\tau,x) + \hat{A}w(\tau,x), \text{ where}$$

$$\hat{A}w(\tau,x) = -\int_{-\infty}^{\infty} \left(w(\tau,x+z) - w(\tau,x) - w_x(\tau,x)(e^z-1)\right) k(z,x)dz;$$

$$w(0,x) = h(x).$$

3.3.1 Variational Formulation

We note that the instantaneous dynamics of the space scaled process are dependent on the level of the underlying stock price through the Lévy system density $k(z,x)$. Thus the elliptical operator A loses its space invariant property. As a consequence, we cannot reduce the case of positive interest and dividend rates to that of zero drift. As mentioned above, the asymptote of the price for a payoff function $h(x)$ is given by $e^{-r\tau}h(x+(r-q)\tau)$. We solve for $u(\tau,\cdot) = w(\tau,\cdot) - h(\cdot+(r-q)\tau)e^{-r\tau}$. This gives us the PIDE for the space scaled process:

$$u_\tau(\tau,\cdot) + Au(\tau,\cdot) = -e^{-r\tau}\hat{A}h(\cdot+(r-q)\tau)$$

We multiply both sides with our usual test function $v(x) \in C_0^\infty$ and integrate to get the variational form

$$(u_\tau(x), v(x)) + (Au(x), v(x)) = -e^{-r\tau}(\hat{A}h(\cdot + (r-q)\tau), v(x))$$

We will describe the work around this problem in order to minimize the computational burden.

3.3.2 Discretization of the PIDE

We discretize the PIDE for space scaled processes in the same way as the PIDE for Lévy processes. This gives us the matrix equation for the FEM solution:

$$\Delta\tau^{-1}(Mu^m - Mu^{m-1}) + \theta Au^m + (1-\theta)Au^{m-1} = F_\tau, \tag{3.8}$$

$$u^m = ((M + \Delta\tau\theta A))^{-1}\left(Mu^{m-1} + \Delta\tau F - \Delta t(1-\theta)Au^{m-1}\right)$$

$$M_{ij} = (\phi_j, \phi_i);$$

$$A_{ij} = \tilde{a}(\phi_j, \phi_i);$$

$$F_\tau^i = -(e^{-r\tau}\hat{A}h(\cdot + (r-q)\tau), \phi_i).$$

3.3.3 Two Stage PIDE solution for VIX

We can solve the pricing PIDE (3.7) numerically with $h(x) = x$ from $T + h$ to time T to get $e^{-rh}E_T\left[\ln(S_{T+h})\right]$. We use the solution in (1.8) to approximate V_T. We then solve a second PIDE with $h(x) = (V_T - K)^+$ or $(K - V_T)^+$ to get prices for calls and

puts on the square-root of VIX. Our method of choice for solving the PIDEs is the Finite Element Method (FEM).

3.4 Computation of the stiffness matrix

We compute the stiffness matrix $A_{ij} = (A\phi_j, \phi_i)$ in two parts. We first compute $A\phi_j(x)$ for each j. We then compute the outer integral $(A\phi_j, \phi_i)$ through quadrature. We start by proving a lemma and a theorem which will help us in computing $A\phi_j(x)$.

Lemma 2 *Let* $\tilde{M} = M/a(x)$, $\tilde{G} = G/a(x)$, *and* $0 \leq Y < 2$, *then*

(i) $\lim_{z \longrightarrow 0^+} z^{-Y} \left(e^{-(\tilde{M}-1)z} - e^{-\tilde{M}z} - ze^{-\tilde{M}z} \right) = 0$

(ii) $\lim_{z \longrightarrow 0^+} z^{1-Y} \left(-\left(\tilde{M}-1\right) e^{-(\tilde{M}-1)z} + \tilde{M}e^{-\tilde{M}z}(1+z) - e^{-\tilde{M}z} \right) = 0$

(iii) $\lim_{z \longrightarrow 0-} y^{-Y} \left(e^{-(\tilde{G}+1)y} - e^{-\tilde{G}y} + ye^{-\tilde{G}y} \right) = 0$

(iv) $\lim_{z \longrightarrow 0-} y^{1-Y} \left(-\left(\tilde{G}+1\right) e^{-(\tilde{G}+1)y} - \tilde{G}e^{-\tilde{G}y}(y-1) + e^{-\tilde{G}y} \right) = 0$

Proof.

(i) Using Taylor expansion we see that

$$\begin{aligned}
& \lim_{z \longrightarrow 0^+} z^{-Y} \left(e^{-(\tilde{M}-1)z} - e^{-\tilde{M}z} - ze^{-\tilde{M}z} \right) \\
= & \lim_{z \longrightarrow 0^+} z^{-Y} 1 - (\tilde{M}-1)z + (\tilde{M}-1)^2 z^2/2 \\
& -(1 - \tilde{M}z + \tilde{M}^2 z^2/2) - z + \tilde{M}z^2 + +o(z^3)) \\
= & \lim_{z \longrightarrow 0^+} ((2\tilde{M}^2 - 1/2)z^{2-Y} + o(z^{3-Y}) \\
= & \ 0 \ \text{ as } Y < 2.
\end{aligned}$$

(ii) By Taylor expansion

$$
\begin{aligned}
& \lim_{z \longrightarrow 0^+} z^{1-Y} \left(- \left(\tilde{M} - 1 \right) e^{-(\tilde{M}-1)z} + \tilde{M} e^{-\tilde{M}z} (1+z) - e^{-\tilde{M}z} \right) \\
= & \lim_{z \longrightarrow 0^+} z^{1-Y} (- \left(\tilde{M} - 1 \right) + \left(\tilde{M} - 1 \right)^2 z + (\tilde{M} - \tilde{M}^2 z)(1+z) \\
& -(1 - \tilde{M}z) + o(z^2)) \\
= & \lim_{z \longrightarrow 0^+} z^{1-Y} (\left(\tilde{M} - 1 \right)^2 z - \tilde{M}^2 z + 2\tilde{M}z + o(z^2)) \\
= & \lim_{z \longrightarrow 0^+} z^{2-Y} + o(z^{3-Y}) \\
= & \ 0 \ \text{ as } Y < 2.
\end{aligned}
$$

(iii) By Taylor expansion

$$
\begin{aligned}
& \lim_{z \longrightarrow 0-} y^{-Y} \left(e^{-(\tilde{G}+1)y} - e^{-\tilde{G}y} + y e^{-\tilde{G}y} \right) \\
= & \lim_{z \longrightarrow 0-} y^{-Y} (1 - (\tilde{G}+1)y + (\tilde{G}+1)^2 y^2/2 - (1 - \tilde{G}y + \tilde{G}^2 y^2/2) \\
& + y(1 - \tilde{G}y) + o(y^3)) \\
= & \lim_{z \longrightarrow 0-} y^{-Y} \left((\tilde{G}+1)^2 y^2/2 - (\tilde{G}^2 y^2/2) + y(\tilde{G}y) + o(y^3) \right) \\
= & \lim_{z \longrightarrow 0-} y^{2-Y}/2 + o(y^{3-Y}) \\
= & \ 0 \ \text{ as } Y < 2.
\end{aligned}
$$

(iv) By Taylor expansion

$$\begin{aligned}
& \lim_{z\longrightarrow 0-} y^{1-Y}\left(-\left(\tilde{G}+1\right)e^{-(\tilde{G}+1)y}-\tilde{G}e^{-\tilde{G}y}(y-1)+e^{-\tilde{G}y}\right) \\
= & \lim_{z\longrightarrow 0-} y^{1-Y}(-\left(\tilde{G}+1\right)+(\tilde{G}+1)^2y)-(\tilde{G}-\tilde{G}^2y)(y-1) \\
& +(1-\tilde{G}y)+o(y^2)) \\
= & \lim_{z\longrightarrow 0-} y^{2-Y}+o(y^{3-Y}) \\
= & \ 0 \ \text{ as } Y<2.
\end{aligned}$$

■

Theorem 3 *Let $k(z,x)$ be the Lévy system density of a scaled CGMY process and let $\tilde{M}$ and $\tilde{G}$ be as defined above. Define $W(x) := \int_{-\infty}^{\infty}(e^z-1-z)k(z,x)dz$. Then*

$$W(x) = Ca(x)^Y \frac{\Gamma(2-Y)}{Y(Y-1)}\times$$
$$\left[\left(\tilde{G}+1\right)^Y-\tilde{G}^{Y-1}\left(\tilde{G}+Y\right)+\left(\tilde{M}-1\right)^Y-\tilde{M}^{Y-1}\left(\tilde{M}-Y\right)\right].$$

Proof. We look at two cases, $z>0$ and $z<0$.

Case 1**:** $z>0$

Consider the integral

$$
\begin{aligned}
I_1(a) &= \int_a^\infty (e^z - 1 - z)k(z,x)dz \\
&= \int_a^\infty (e^z - 1 - z)Ca(x)^Y e^{-\tilde{M}z} z^{-1-Y} dz \\
&= Ca(x)^Y \frac{z^{-Y}}{-Y}\left(e^{-(\tilde{M}-1)z} - e^{-\tilde{M}z} - ze^{-\tilde{M}z}\right)\Big|_a^\infty \\
&- \int_a^\infty Ca(x)^Y \frac{z^{-Y}}{-Y}\left(-\left(\tilde{M}-1\right)e^{-(\tilde{M}-1)z} + \tilde{M}e^{-\tilde{M}z}(1+z) - e^{-\tilde{M}z}\right)dz \\
&= Ca(x)^Y \frac{z^{-Y}}{-Y}\left(e^{-(\tilde{M}-1)z} - e^{-\tilde{M}z} - ze^{-\tilde{M}z}\right)\Big|_a^\infty \\
&+ \frac{Ca(x)^Y}{Y}\int_a^\infty z^{-Y}\left(-\left(\tilde{M}-1\right)e^{-(\tilde{M}-1)z} + \tilde{M}e^{-\tilde{M}z}(1+z) - e^{-\tilde{M}z}\right)dz \\
&= Ca(x)^Y \frac{z^{-Y}}{-Y}\left(e^{-(\tilde{M}-1)z} - e^{-\tilde{M}z} - ze^{-\tilde{M}z}\right)\Big|_a^\infty \\
&+ \frac{Ca(x)^Y}{Y}\left[\frac{z^{1-Y}}{(1-Y)}\left(-\left(\tilde{M}-1\right)e^{-(\tilde{M}-1)z} + \tilde{M}e^{-\tilde{M}z}(1+z) - e^{-\tilde{M}z}\right)\Big|_a^\infty\right] \\
&- \frac{Ca(x)^Y}{Y(1-Y)}\int_a^\infty z^{1-Y}\left(-\left(\tilde{M}-1\right)^2 e^{-(\tilde{M}-1)z} - \tilde{M}^2 e^{-\tilde{M}z}(1+z) + 2\tilde{M}e^{-\tilde{M}z}\right)dz.
\end{aligned}
$$

Letting $a \longrightarrow 0_+$ and using Lemma (2) above, we get

$$
\begin{aligned}
I_1(0) &= \lim_{a \longrightarrow 0_+} I_1(a) \\
&= \frac{Ca(x)^Y}{Y(Y-1)}\int_0^\infty z^{1-Y}\left(-\left(\tilde{M}-1\right)^2 e^{-(\tilde{M}-1)z} - \tilde{M}^2 e^{-\tilde{M}z}(1+z) + 2\tilde{M}e^{-\tilde{M}z}\right)dz \\
&= \frac{Ca(x)^Y}{Y(Y-1)}\Gamma(2-Y)\left((M-1)^Y - M^{Y-1}(M-Y)\right)
\end{aligned}
$$

Case 2**:** $z < 0$

Consider the integral

$$
\begin{aligned}
I_2(b) &= \int_{-\infty}^{b} (e^z - 1 - z)k(z,x)dz \\
&= \int_{-\infty}^{b} (e^z - 1 - z)Ca(x)^Y e^{\tilde{G}z}(-z)^{-1-Y}dz. \text{ Let } y = -z. \text{ Then} \\
I_2(b) &= \int_{b}^{\infty} (e^{-((\tilde{G}+1)y} - e^{-\tilde{G}y} + ye^{-\tilde{G}y})Ca(x)^Y y^{-1-Y}dy \\
&= Ca(x)^Y \frac{y^{-Y}}{-Y}\left(e^{(\tilde{G}+1)y} - e^{\tilde{G}y} + ye^{\tilde{G}y}\right)\Big|_b^{\infty} \\
&- Ca(x)^Y \int_b^{\infty} \frac{y^{-Y}}{-Y}\left(-\left(\tilde{G}+1\right)e^{-(\tilde{G}+1)y} - \tilde{G}e^{-\tilde{G}z}(y-1) + e^{-\tilde{G}y}\right)dy \\
&= Ca(x)^Y \frac{y^{-Y}}{-Y}\left(e^{(\tilde{G}+1)y} - e^{\tilde{G}y} + ye^{\tilde{G}y}\right)\Big|_b^{\infty} \\
&+ Ca(x)^Y \frac{y^{1-Y}}{Y(1-Y)}\left(-\left(\tilde{G}+1\right)e^{-(\tilde{G}+1)y} - \tilde{G}e^{-\tilde{G}z}(y-1) + e^{-\tilde{G}y}\right)\Big|_b^{\infty} dy \\
&- Ca(x)^Y \int_b^{\infty} \frac{y^{1-Y}}{Y(1-Y)}\left(\left(\tilde{G}+1\right)^2 e^{-(\tilde{G}+1)y} + \tilde{G}^2 e^{-\tilde{G}z}(y-1) - 2\tilde{G}e^{-\tilde{G}y}\right)dy.
\end{aligned}
$$

Letting $b \longrightarrow 0_-$ and again using Lemma (2) above,

$$
\begin{aligned}
I_2(0) &= \lim_{b \longrightarrow 0_-} I_2(b) \\
&= Ca(x)^Y \int_b^{\infty} \frac{y^{1-Y}}{Y(Y-1)}\left(\left(\tilde{G}+1\right)^2 e^{-(\tilde{G}+1)y} + \tilde{G}^2 e^{-\tilde{G}z}(y-1) - 2\tilde{G}e^{-\tilde{G}y}\right)dy \\
&= \frac{Ca(x)^Y}{Y(Y-1)}\Gamma(2-Y)\left(\left(\tilde{G}+1\right)^Y - \tilde{G}^{Y-1}\left(\tilde{G}+Y\right)\right).
\end{aligned}
$$

This completes the proof since $W(x) = I_1(0) + I_2(0)$. ■

We note that since $a(x) > 0$, $W(x)$ is free of non-integrable singularities.

3.4.1 Jump Operator Applied to Hat Functions

Now that we have a closed form non-singular solution of $W(x)$, we look at the integral part $\widehat{A}u(x)$ of the PIDE operator in equation (3.7) applied to the hat function ϕ_j

$$\widehat{A}\phi_j(x) := \int_{-\infty}^{\infty} \Big(\phi_j(x+z) - \phi_j(x) - \phi_j^{'}(x)(e^z - 1)\Big)\, k(z,x)dz. \tag{3.9}$$

Case 1**:** $x \in (x_{j-1}, x_j)$.

$$\begin{aligned}\widehat{A}\phi_j(x) = \int_{-\infty}^{\infty} \Big(\Big(\phi_j(x+z) - \phi_j(x) - \phi_j^{'}(x)z\Big)\Big)\, k(z,x)dz \\ -\phi_j^{'}(x)\int_{-\infty}^{\infty}(e^z - 1 - z)\, k(z,x)dz \\ = I_2 - I_1.\end{aligned} \tag{3.10}$$

$$\begin{aligned} I_2 \;=\; & \left(\left(\frac{x_{j-1}}{h_j} + \frac{x_{j+1}}{h_{j+1}}\right) - x\left(\frac{1}{h_j} + \frac{1}{h_{j+1}}\right)\right)\int_{x_j - x}^{x_{j+1}-x} k(z,x)dz \\ & - \left(\frac{1}{h_j} + \frac{1}{h_{j+1}}\right)\int_{x_j-x}^{x_{j+1}-x} zk(z,x)dz \\ & - \left(\frac{x - x_{j-1}}{h_j}\right)\int_{-\infty}^{x_j - x} k(z,x)dz - \frac{1}{h_j}\int_{-\infty}^{x_{j-1}-x} zk(z,x)dz \\ & - \left(\frac{x - x_{j-1}}{h_j}\right)\int_{x_{j+1}-x}^{\infty} k(z,x)dz - \frac{1}{h_{j+1}}\int_{x_{j+1}-x}^{\infty} zk(z,x)dz, \end{aligned} \tag{3.11}$$

$$I_1 = -\phi_j^{'}(x)W(x), \tag{3.12}$$

$$I_1 = -\phi_j^{'}(x)W(x), \tag{3.13}$$

Case 2: $x \in (x_j, x_{j+1})$.

$$\begin{aligned}\widehat{A}\phi_j(x) = \int_{-\infty}^{\infty} \Big(\Big(\phi_j(x+z) - \phi_j(x) - \phi_j^{'}(x) z \Big) \Big) \, k(z,x) dz \\ -\phi_j^{'}(x) \int_{-\infty}^{\infty} (e^z - 1 - z) \, k(z,x) dz \\ = I_3 - I_1.\end{aligned} \tag{3.14}$$

$$\begin{aligned} I_3 \;=\; & x \left(\frac{1}{h_j} + \frac{1}{h_{j+1}} \right) \int_{x_{j-1}-x}^{x_j - x} k(z,x) dz - \\ & \left(\frac{x_{j-1}}{h_j} + \frac{x_{j+1}}{h_{j+1}} \right) \int_{x_{j-1}-x}^{x_j - x} k(z,x) dz + \left(\frac{1}{h_j} + \frac{1}{h_{j+1}} \right) \int_{x_{j-1}-x}^{x_j - x} z k(z,x) dz \\ & - \left(\frac{x_{j+1} - x}{h_{j+1}} \right) \int_{-\infty}^{x_{j-1}-x} k(z,x) dz + \frac{1}{h_{j+1}} \int_{-\infty}^{x_{j-1}-x} z k(z,x) dz \\ & - \left(\frac{x_{j+1} - x}{h_{j+1}} \right) \int_{x_{j+1}-x}^{\infty} k(z,x) dz + \frac{1}{h_{j+1}} \int_{x_{j+1}-x}^{\infty} z k(z,x) dz. \end{aligned} \tag{3.15}$$

Case 3: $x < x_{j-1}$ **or** $x > x_{j+1}$

$$\begin{aligned}\widehat{A}\phi_j(x) = \int_{-\infty}^{\infty} \Big(\Big(\phi_j(x+z) - \phi_j(x) - \phi_j^{'}(x) z \Big) \Big) \, k(z,x) dz \\ -\phi_j^{'}(x) \int_{-\infty}^{\infty} (e^z - 1 - z) \, k(z,x) dz \\ = I_4 - I_1.\end{aligned} \tag{3.16}$$

$$\begin{aligned} I_4 \;=\; & \left(\frac{x - x_{j-1}}{h_j} \right) \int_{x_{j-1}-x}^{x_j - x} k(z,x) dz + \left(\frac{x_{j+1} - x}{h_{j+1}} \right) \int_{x_j - x}^{x_{j+1} - x} k(z,x) dz \\ & + \frac{1}{h_j} \int_{x_{j-1}-x}^{x_j - x} z k(z,x) dz - \frac{1}{h_{j+1}} \int_{x_j - x}^{x_{j+1} - x} z k(z,x) dz. \end{aligned} \tag{3.17}$$

Note that all the integrals in the cases above are of the type $\int_a^b k(z,x)dz$ or $\int_a^b zk(z,x)dz$, where $a, b \in [-\infty, \infty]$. To solve these integrals, we define the first and second tail integrals of the Lévy and Lévy-SSL densities as

$$K_{-1}(z,x) \;:=\; \begin{cases} -\int_z^\infty k(s,x)ds & \text{if } z>0, \\ \int_{-\infty}^z k(s,x)ds & \text{if } z<0 \end{cases}, \tag{3.18}$$

$$K_{-2}(z,x) \;:=\; \begin{cases} -\int_z^\infty K_{-1}(s,x)ds & \text{if } z>0, \\ \int_{-\infty}^z K_{-1}(s,x)ds & \text{if } z<0. \end{cases}.$$

We note that these tail integrals are precisely the first and second anti-derivatives of the Lévy density. These anti-derivatives vanish at $z = \pm\infty$. Given this fact, we can easily solve the above integrals as

$$\begin{aligned} \int_a^b k(z,x)dz &= K_{-1}(b,x) - K_{-1}(a,x) \\ \int_a^b zk(z,x)dz &= bK_{-1}(b,x) \\ &\quad -aK_{-1}(a,x) - (K_{-2}(b,x) - K_{-2}(a,x)). \end{aligned} \tag{3.19}$$

3.4.2 Tail integrals of CGMY and CGMYSSL Lévy system densities.

We define a Matlab implementable function similar to an incomplete gamma function by

$$\tilde{\Gamma}(x,\alpha,G) = \int_x^\infty z^{\alpha-1}e^{-Gz}dz. \tag{3.20}$$

We use this function to calculate the derivatives of the CGMY process

Theorem 4 *The first and second tail integrals of the CGMYSSL process are given by*

$$K_{-1}(z,x) = \begin{cases} -a(x)^Y \frac{C}{Y} z^{-Y} e^{-\tilde{M}z} - a(x)^Y \frac{C\tilde{M}}{Y(1-Y)} z^{1-Y} e^{-\tilde{M}z} \\ \qquad +a(x)^Y \frac{C\tilde{M}^2}{Y(1-Y)} \tilde{\Gamma}(z, 2-Y, \tilde{M})). & \text{if } z > 0 \\ a(x)^Y \frac{C}{Y} (|z|^{-Y} e^{-\tilde{G}|z|} - \tilde{G}\tilde{\Gamma}(|z|, 1-Y, \tilde{G})) \text{ if } z < 0, \end{cases} \tag{3.21}$$

$$\tilde{M} = \min(M/a(x), 1) \text{ and } \tilde{G} = \min(G/a(x), 1).$$

$$K_{-2}(z,x) = \begin{cases} \frac{C}{\tilde{M}} a(x)^Y z^{-Y} e^{-\tilde{M}z} + (Y/\tilde{M} + z) K_{-1}(z,x) & \text{if } z > 0 \\ (z - Y/\tilde{G}) K_{-1}(z,x) + \frac{C}{\tilde{G}} a(x)^Y (-z)^{-Y} e^{\tilde{G}z} & \text{if } z < 0. \end{cases}$$

Proof. Case 1**:** $z > 0$

Integrating by parts twice, we get

$$\begin{aligned} K_{-1}(z,x) \quad : \quad &= -\int_z^\infty k(s,x) ds \\ &= -Ca(x)^Y \int_z^\infty e^{-\tilde{M}s} s^{-1-Y} ds \\ &= -Ca(x)^Y \left(e^{-\tilde{M}s} \frac{s^{-Y}}{-Y} \Big|_z^\infty - \frac{\tilde{M}}{Y} \int_z^\infty e^{-Ms} s^{-Y} ds \right) \\ &= -a(x)^Y \frac{C}{Y} z^{-Y} e^{-\tilde{M}z} - a(x)^Y \frac{C\tilde{M}}{Y(1-Y)} z^{1-Y} e^{-\tilde{M}z} \\ &\quad +a(x)^Y \frac{C\tilde{M}^2}{Y(1-Y)} \int_z^\infty s^{1-Y} e^{-\tilde{M}s} ds \\ &= -a(x)^Y \frac{C}{Y} z^{-Y} e^{-\tilde{M}z} - a(x)^Y \frac{C\tilde{M}}{Y(1-Y)} z^{1-Y} e^{-\tilde{M}z} \\ &\quad +a(x)^Y \frac{C\tilde{M}^2}{Y(1-Y)} \tilde{\Gamma}(z, 2-Y, \tilde{M})). \end{aligned} \tag{3.22}$$

Since $Y < 2$, the function $\tilde{\Gamma}$ has an integrable singularity at zero.

By definition of $K_{-1}(z,x)$,

$$\begin{aligned}
K_{-2}(z,x) &:= -\int_z^\infty K_{-1}(t,x)dt \\
&= Ca(x)^Y \int_{t=z}^\infty \int_{s=t}^\infty s^{-Y-1}e^{-\tilde{M}s}dsdt \\
&= Ca(x)^Y \int_{s=z}^\infty \int_{t=z}^s s^{-Y-1}e^{-\tilde{M}s}dtds \\
&= Ca(x)^Y \left(\int_z^\infty s^{-Y}e^{-\tilde{M}s}ds - z\int_s^\infty e^{-Ms}s^{-Y}ds \right) \\
&= Ca(x)^Y \left(s^{-Y}\frac{e^{-\tilde{M}s}}{-\tilde{M}}\bigg|_z^\infty - \frac{Y}{\tilde{M}}\int_z^\infty s^{-Y-1}e^{-\tilde{M}s}ds + zK_{-1}(z,x) \right) \\
&= \frac{C}{\tilde{M}}a(x)^Y z^{-Y}e^{-\tilde{M}z} + \frac{Y}{\tilde{M}}K_{-1}(z,x) + zK_{-1}(z,x) \\
&= \frac{C}{\tilde{M}}a(x)^Y z^{-Y}e^{-\tilde{M}z} + \left(\frac{Y}{\tilde{M}} + z\right)K_{-1}(z,x). \qquad (3.23)
\end{aligned}$$

Case 2: $z < 0$

$$\begin{aligned}
K_{-1}(z,x) &:= \int_{-\infty}^z k(s,x)ds \\
&= Ca(x)^Y \int_{-\infty}^z e^{\tilde{G}s}(-s)^{-1-Y}ds \\
&= \int_{-z}^\infty e^{-\tilde{G}t}t^{-1-Y}dt \\
&= -K_{-1}(-z,x) \qquad (3.24)
\end{aligned}$$

By case 1,

$$\begin{aligned}
K_{-1}(z,x) &= a(x)^Y \frac{C}{Y}(-z)^{-Y}e^{\tilde{G}z} + a(x)^Y \frac{C\tilde{G}}{Y(1-Y)}(-z)^{1-Y}e^{\tilde{G}z} \\
&\quad -a(x)^Y \frac{C\tilde{G}^2}{Y(1-Y)}\tilde{\Gamma}(-z, 2-Y, \tilde{G})).
\end{aligned}$$

For $K_{-2}(z,x)$

$$\begin{aligned} K_{-2}(z,x) \quad &: \quad = \int_{-\infty}^{z} K_{-1}(t,x)dt \\ &\quad - \int_{-\infty}^{z} K_{-1}(-t,x)dt \\ &= \quad - \int_{-z}^{\infty} K_{-1}(s,x)ds \\ &= \quad \frac{C}{\tilde{G}} a(x)^{Y}(-z)^{-Y} e^{\tilde{G}z} + \left(\frac{Y}{\tilde{G}} - z\right) K_{-1}(-z,x) \\ &\quad \frac{C}{\tilde{G}} a(x)^{Y}(-z)^{-Y} e^{\tilde{G}z} + \left(z - \frac{Y}{\tilde{G}}\right) K_{-1}(z,x). \end{aligned} \tag{3.25}$$

The last step follows from eqn (3.24). ■

3.5 RHS Vector for the Linear Equation

3.5.1 RHS function for call option payoff

We need the RHS $F_i(t) = -(e^{-rt}\hat{A}h(x+(r-q)t), \phi_i(x))$ for our FEM algorithm. We show that the RHS can be reduced to a simple form where the formulae and methods derived to calculate the stiffness matrix can be efficiently applied for calculations.

Lemma 5 *Define* $\psi(\cdot; K, r, q, \tau) := \hat{A}h(\cdot + (r-q)\tau; K)$, *for* $h(x;K) = (\exp(x) - K)^{+}$. *Here* $\hat{A}$ *is the pure jump operator defined above. Let* $r = 0$ *and* $q = 0$. *Then*

$\psi(x;K,0,0,\tau)$ for the CGMYSSL process is given by

$$\psi(x;K,0,0,\tau) = \begin{cases} e^x K_{-1}(\ln K - x; M/a(x) - 1) \\ -K K_{-1}(\ln K - x; M/a(x)) \quad \textit{when } x < \ln K \\ e^x K_{-1}\left(\ln K - x; G/a(x) + 1\right) \\ -K K_{-1}\left(\ln K - x; G/a(x)\right) \quad \textit{when } x > \ln K \end{cases}$$

Proof. Case 1**:** $x < \ln K$

In this case, $h(x) = 0$ and $h'(x) = 0$. Let $\tilde{M} = M/a(x)$ and $\tilde{G} = G/a(x)$. Then

$$\psi(x;K,0,0,\tau) := \hat{A}h(x;K)$$

$$= -\int_{-\infty}^{\infty} \left(h(x+z) - h(x) - (e^z - 1)h^{'}(x)\right) k(z,x)dz$$

$$\begin{aligned} &= -\int_{\ln K - x}^{\infty} \left(e^{x+z} - K\right) k(z,x)dz \\ &= -\int_{\ln K - x}^{\infty} \left(e^{x+z} - K\right) Ca(x)^Y e^{-Mz/a(x)} z^{-1-Y} dz \\ &= -e^x Ca(x)^Y \int_{\ln K - x}^{\infty} e^{-(\tilde{M}-1)z} z^{-1-Y} dz \\ &\quad + KCa(x)^Y \int_{\ln K - x}^{\infty} e^{-\tilde{M}z} z^{-1-Y} dz \\ &= e^x K_{-1}(\ln K - x; \tilde{M} - 1) - K K_{-1}(\ln K - x; \tilde{M}). \end{aligned}$$

Case 2: $x > \ln K$

In this case, $h(x) = e^x - K$ and $h'(x) = e^x$.

$$\psi(x;K,0,0,\tau) := \hat{A}h(x;K)$$
$$-\int_{-\infty}^{\infty}\left(h(x+z)-h(x)-(e^z-1)h^{'}(x)\right)k(z,x)dz$$
$$=\int_{-\infty}^{\ln K-x}\int_{\ln K-x}^{0}\int_{0}^{\infty}\left(h(x+z)-h(x)-(e^z-1)h^{'}(x)\right)k(z,x)dz.$$
$$=\int_{-\infty}^{\ln K-x}\left(0-(e^x-K)-(e^z-1)e^x\right)k(z,x)dz$$
$$+\int_{\ln K-x}^{0}\int_{0}^{\infty}\left(\left(e^{x+z}-K\right)-(e^x-K)-(e^z-1)e^x\right)k(z,x)dz$$

$$\begin{aligned}
&= \int_{-\infty}^{\ln K-x}\left(e^{x+z}-K\right)Ca(x)^Y e^{Gz/a(x)}(-z)^{-1-Y}dz \\
&= e^x Ca(x)^Y\int_{-\infty}^{\ln K-x}e^{(G/a(x)+1)z}(-z)^{-1-Y}dz \\
&\quad -KCa(x)^Y\int_{-\infty}^{\ln K-x}e^{Gz/a(x)}(-z)^{-1-Y}dz \\
&= e^x K_{-1}\left(\ln K-x;\frac{G}{a(x)}+1\right)-KK_{-1}\left(\ln K-x;\frac{G}{a(x)}\right).
\end{aligned}$$

■

Lemma 6 *Let $r>0$ and $q>0$. Then for the $\psi(x;K,r,q,\tau)$ is given by*

$$\psi(x;K,r,q) = e^{-qt}\psi(x;K,0,0)$$

Proof.

$$h(x+(r-q)\tau;K). = \left(e^{x+(r-q)\tau} - K\right)^+$$

$$= e^{(r-q)\tau}\left(e^x - Ke^{-(r-q)\tau}\right)^+$$

$$= e^{(r-q)\tau}h(x;Ke^{-(r-q)\tau}). \text{ Now}$$

$$\begin{aligned}
\psi(x;r) &= -\int_{-\infty}^{\infty}(h(x+(r-q)\tau+z;K) - h(x+(r-q)\tau;K) \\
&\quad -(e^z-1)h^{'}(x+(r-q)\tau;K))k(z,x)dz \\
&= -e^{(r-q)\tau}\int_{-\infty}^{\infty}(h(x+z;Ke^{-(r-q)\tau}) - h(x;Ke^{-(r-q)\tau}) \\
&\quad -(e^z-1)h^{'}(x;Ke^{-(r-q)\tau}))k(z,x)dz \\
&= e^{(r-q)\tau}\hat{A}h(x;Ke^{-(r-q)\tau}).
\end{aligned}$$

■

These two lemmas directly give us the following theorem:

Theorem 7 *Let $r > 0$. The RHS $F_i(\tau) = -(e^{-rt}\hat{A}h(x+(r-q)\tau), \phi_i(x))$ for the CGMY process is given by*

$$F_i(t) = (e^{-qt}\hat{A}_0 h(x;Ke^{-(r-q)t}), \phi_i(x)).$$

This theorem is very useful in simplifying the generation of the time dependent RHS. Now we can get the RHS simply by using the formulae for $r = 0$, applied to a payoff function with a different strike.

3.5.2 RHS for log payoff

Theorem 8 *Let $\psi(x; r, q, \tau)$ be defined as above for $h(x) = x$, where $x = \ln S$. Then the RHS function $F_i(\tau) = -(e^{-r\tau}\psi(x; r, q, \tau), \phi_i(x))$ is given by*

$$F_i(\tau) = -(e^{-r\tau}W(x), \phi_i(x)).$$

Proof.

$$\begin{aligned}
\psi(x; r, q, \tau) &= \hat{A}h(x + (r - q)\tau) \\
&= -\int_{-\infty}^{\infty} (h(x + (r - q)\tau + z) - h(x + (r - q)\tau) \\
&\quad -(e^z - 1)h'(x + (r - q)\tau))k(z, x)dz \\
&= -\int_{-\infty}^{\infty} ((x + (r - q)\tau + z - (x + (r - q)\tau) - (e^z - 1))\, k(z, x)dz \\
&= \int_{-\infty}^{\infty} (e^z - 1 - z)\, k(z, x)dz \\
&= W(x).
\end{aligned}$$

■

The result follows directly from the above equality.

3.5.3 RHS for derivatives of VIX

Theorem 9 *Let $\psi(x;r,q,\tau)$ be defined as above for $h(x)=\sum_{j=1}^{N}\alpha_j\phi_j(x)$. Then the RHS function $F_i(\tau)=-(e^{-r\tau}\psi(x;r,q,\tau),\phi_i(x))$ is given by*

$$e^{-r\tau}\sum_{j=1}^{N}\beta_j(\hat{A}\phi_j(x),\phi_i(x)), \tag{3.26}$$

$$\textit{where}\quad \beta_i=h(x_j+(r-q)\tau).$$

Proof.

$$\begin{aligned}
\psi(x;r,q,\tau) &= \hat{A}h(x+(r-q)\tau)\\
&= -\int_{-\infty}^{\infty}(h(x+(r-q)\tau+z)-h(x+(r-q)\tau)\\
&\quad -(e^z-1)h^{'}(x+(r-q)\tau))k(z,x)dz\\
&= -\int_{-\infty}^{\infty}\sum_{j=1}^{N}\alpha_j\phi_j(x+(r-q)\tau+z)k(z,x)dz\\
&\quad -\int_{-\infty}^{\infty}\sum_{j=1}^{N}\alpha_j\phi_j(x+(r-q)\tau)k(z,x)dz\\
&\quad -\int_{-\infty}^{\infty}(e^z-1)\sum_{j=1}^{N}\alpha_j\phi_j^{'}(x+(r-q)\tau)k(z,x)dz\\
&= -\int_{-\infty}^{\infty}\sum_{j=1}^{N}\beta_j\left(\phi_j(x+z)-\phi_j(x)-(e^z-1)\phi_j^{'}(x)\right)k(z,x)dz.\\
&= -\sum_{j=1}^{N}\beta_j\hat{A}\phi_j(x).
\end{aligned}$$

Here we note that $\alpha_j=h(x_j)$. Since $h(x)$ is a piece-wise linear function, its translation by $(r-q)\tau$ is also a piece-wise linear function with coefficients $\beta_i=h(x_j+(r-q)\tau)$.

Thus

$$\begin{aligned} F_i(\tau) &= -(e^{-r\tau}\psi(x;r,q,\tau),\phi_i(x)) \\ &= e^{-r\tau}\left(\sum_{j=1}^{N}\beta_j\hat{A}\phi_j(x),\phi_i(x)\right) \\ &= e^{-r\tau}\sum_{j=1}^{N}\beta_j(\hat{A}\phi_j(x),\phi_i(x)). \end{aligned}$$

■

Like the above results, this result simplifies the RHS computation for the second stage of the VIX PIDE. Since the VIX index is computed as a piece-wise linear function, the above result applies. We note that the inner product $(\hat{A}\phi_j(x),\phi_i(x))$ is already calculated for the jump component of the stiffness matrix. Thus the RHS computation in this case boils down to a matrix-vector multiplication of the stiffness matrix and the coefficient vector $\beta = \left\{\beta_j\right\}$.

3.6 Geometric Quadrature and Outer Integration

While we could find closed form formulae of the jump operator applied to that hat functions, we need to compute another outer integral $(\phi_i(x), A\phi_j(x))$ to get the stiffness matrix of our finite element scheme. However, we note that the function $A\phi_j(x)$ is singular at three points, $x_{j-1,}x_j$ and x_{j+1}. We note that there is no closed form solution of the outer integral because of the functional form of $A\phi_j(x)$. Our aim was to come up with a good numerical scheme to calculate this outer integral which can integrate near singularities. A benefit of a numerical scheme is that it is easily

portable to another Lévy process. We chose the methodology formulated in Schwab [52] for numerical quadrature of integrals near singularity.

To understand the main idea, assume that we have to integrate a continuous integral which contains a singularity at the right end point. We subdivide the integral into left and right sub intervals such that the length of the singular subinterval (interval containing the singularity) to the non-singular subinterval is close to 0, say .1. We then use regular Gaussian quadrature on the left subinterval with n points (we use $n = 15$). For the right subinterval, since it contains the singularity, we further subdivide it into left and right subintervals such that the new left subinterval is singularity free and the new right interval contains the singularity at the right end point. In other words, we repeat the same subdivision scheme on the right subinterval which contains the singularity at each iteration. One continues to apply Gaussian scheme with $n = q(l)$ points, with l being the level of iterations for some function q. One can continue this scheme for a fixed number of iterations or adaptively, until convergence is reached up to a tolerance level. We choose the later scheme and observe that we rarely go beyond the fifth or sixth level of subdivision. The convergence result in Schwab shows that

Theorem 10 *Let f be an integrable function over an interval Ω, such that f contains an integrable singularity on $\partial\Omega$. Then for every geometric ratio σ, $0 < \sigma < 1$ and a linear degree vector* $\mathbf{p}$

$$p_j = \max\{2, \lfloor j\mu \rfloor + 1\} \quad 2 < j < n + 1$$

with slope $\mu > \gamma_\sigma$, for some γ_σ, there exist constants $b, c > 0$ independent of N such that the convergence of the quadrature scheme $Q_\sigma^{n,\mathbf{p}}$ is exponential, that is,

$$\left| \int_\Omega f(x)dx - Q_\sigma^{n,\mathbf{p}} f \right| \leq c \exp(-bn^{1/3}).$$

Proof. For a proof, see Theorem 4.1 in Schwab [52]. ■

Chapter 4

Numerical Implementation and Results

4.1 Data on VIX and SPX options

We use 70 days of available data on SPX and VIX options from August 22, 2007 to November 29,2007. The SPX data gives option prices for SPX for different maturities ranging from one month to one year, along with the applicable interest and dividend rates for each maturity. We observe that the applicable interest rate is not constant across maturities in the data which is consistent with the observations in the market. Since our PIDE assumes constant interest rates, we work around the interest rate term structure by solving a different PIDE for each maturity. Since the stiffness matrix related to the jump component does not depend on the interest or dividend rates, we only need to compute it once for option prices on a given day. We calibrate our model to out-of-the-money (OTM) options since they are the most liquid. We

also convert the OTM VIX options into in-the-money (ITM) options using put-call parity. The VIX forward prices are provided in the dataset.

4.2 Overview of the Numerical Scheme

Our numerical implementation scheme has two parts. The first part relates to the computation of option prices on SPX and VIX. The second part relates to the calibration algorithm used to calibrate the parameters to the market data on SPX and VIX options. Let us discuss both these parts briefly.

4.2.1 Stage I: Calculation of Option Prices

We have different algorithms for calculating options on SPX and VIX. Let us describe both of them briefly. We start with options on the VIX index

VIX Option Price Calculation

Part (i): For the VIX option prices, we start with a strike price K and a maturity T. We choose a spatial grid vector in log-stock prices. For this grid vector, we compute the mass matrix, the stiffness matrix (see section 3.4) and the RHS function F (see 3.5) for the payoff equal to the log of the stock price ($h(x) := \ln(S)$). We then solve a sequence of matrix equations (3.8) to get the price of the log contract. We plug in this price in equation (1.8) to get the VIX function $V_T(x)$ as a function of the log stock variable x.

Part (ii): We first truncate the function $V_T(x)$ at the boundaries to minimize the

numerical error coming from the boundaries. We take the function $V_T(x)$ obtained in Part (i) above and use it to compute the VIX call option payoff $h(x) := (V_T(x) - K)^+$ or the VIX put option payoff $h(x) := (K - V_T(x))^+$. We are now ready to run a second PIDE. We compute the RHS for this new PIDE for the new payoff function $h(x) := (V_T(x) - K)^+$ or $h(x) := (K - V_T)^+$ (see section 3.4). We use the same stiffness and mass matrices that we calculated in Part (i). We now solve a series of matrix equations (3.8) for the new RHS to obtain the price of VIX options.

SPX Option Price Calculation

This algorithm is simpler than the one for calculating VIX options. We compute the stiffness matrix (see section 3.4) and the RHS function F (see 3.5) for the call option payoff $h(x) := (e^x - K)^+$. We solve the matrix equations (3.8) to obtain call option prices. We price put options using the put call parity

$$CP - PP = Se^{-qT} - Ke^{-rT},$$

where CP is the call price, PP is the put price and the other variables are as defined above.

4.2.2 Stage II: Model Calibration to Market Prices

We use the option prices computed in Stage I above for different strikes and maturities in the Matlab optimization function 'fminunc' to minimize the mean square error between the model and market prices. We use a tolerance setting of $1e^{-6}$ for the

matlab parameters TolX and TolFun. We run three different kinds of calibrations which are described in detail below. Each calibration took about 3-4 hours and around 600 iterations. We realize that this is quite slow for a real-time implementation. However, we note that all the code was written in Matlab and can be easily be made very efficient by coding in C or C++.

4.2.3 General Setting for Numerical Calculations

We perform three different types of calibrations. We first calibrate our model to SPX surface of option prices and also to VIX surface separately. We also do a joint calibration of options on SPX and VIX for a given maturity on a given day. We provide details of our estimation results below. Since the VIX option maturities don't always coincide with the SPX option maturities, we first use a CGMY self-decomposable model (see [10], [15] and [25]) to parametrize the SPX option surface. We then extract SPX option prices to match VIX maturities.

We used 28 degrees of freedom in the PIDE for SPX. The number of degrees of freedom was based on our numerical experiments with different grid sizes. We wanted to optimize the computational speeds without introducing significant errors. We used a uniform grid in stock with a range from \$600 to \$2500. The number of SPX options ranged from 200 to 250 for different days and the number of VIX options ranged from 50 to 100. We eliminated option prices with prices less than $.00075S_0$, to remove illiquid options. We used 6 points for Gaussian quadrature on intervals containing singularity and 15 points for quadrature over other intervals. We use the geometric

ratio for refinement equal to 0.1.

For SPX options, we use 5 time steps for all options. Thus options with longer maturity have bigger time steps. We did this to obtain reasonable computation speeds. Since the initial function has a singularity at the log-strike, we use backward Euler (BE) method for the first two steps to have better accuracy near the singularity. We use Crank-Nicholson scheme for the remaining time steps for faster convergence. Since this changes the LHS matrix, this would normally force us to compute the LU decomposition twice. However, if we make the BE time-steps half the size of the CN time-steps, the LHS matrices remain the same for the BE and CN time steps, thus avoiding the extra LU decomposition.

For VIX Options, we first compute the price of the log contract with 36 degrees of freedom. We use the solution to get VIX index function. We then ignore the three outermost values of VIX function on both sides to avoid errors on the boundary. This reduces our degrees of freedom to 30.

Since there are no singularities in the linear payoff function, we use the CN scheme for faster convergence. We use the log contract solution to generate the payoff functions for options on VIX as described above. We then use CN scheme again with 5 time steps to get the price of options on VIX.

4.3 Reduction in Independent Parameters

We note that even though our model is specified in terms of seven parameters, four CGMY parameters and three scaling parameters, we only have six degrees of freedom.

To see why this is the case, assume without loss of generality that $z > 0$. Then

$$k_{cgmyssl}(z,x) = C\left(\alpha+\beta(x-\xi)^2\right)^Y \exp\left(-\frac{M}{(\alpha+\beta(x-\xi)^2)}z\right) z^{-1-Y} \tag{4.1}$$
$$= C\beta^Y\left(\frac{\alpha}{\beta}+(x-\xi)^2\right)^Y e^{\left(-\frac{M}{\beta\left(\frac{\alpha}{\beta}+(x-\xi)^2\right)}z\right)} z^{-1-Y}$$

Let $\tilde{C} = C\beta^Y$, $\tilde{G} = \frac{G}{\beta}$, $\tilde{M} = \frac{M}{\beta}$, Y, $\tilde{\alpha} = \frac{\alpha}{\beta}$ and ξ. In our calibrations, we freeze $C = 1$ to estimate the six degrees of freedom. We report the other parameters G, M, Y, α, β and ξ.

4.4 Calibration Results

4.4.1 CGMY performance

While we know that time homogenous models are unsuitable for pricing options on VIX as the volatility of volatility in these models is constant, we still calibrate the CGMY model to benchmark the performance of our space-dependent pure jump model. We perform a joint estimation of the SPX and VIX marginal distributions for the same day that was randomly selected above. We report the parameters and the errors for three option maturities in 4.1 below.

We observe that the errors are fairly high for both short and medium term maturities. This result supports our theoretical argument that the CGMY model cannot price the time value of the VIX index. We do the above calibration solely to benchmark the performance of our model.

Date	*Maturity*	*C*	*G*	*M*	*Y*	*errspx*	*errvix*
10/24/07	12/19/07	0.21	4.40	21.31	0.93	11.08%	12.10%
10/24/07	1/16/08	0.71	6.76	23.94	0.58	8.89%	12.94%
10/24/07	3/19/08	0.50	5.34	26.42	0.62	10.26%	16.08%

Table 4.1: This table show the performance of the CGMY model in simultaneously pricing VIX and SPX options of a given maturity. We chose options with three differnt maturities between one month and one year from the market data as of a randomly selected day (10/24/2007) from our dataset. We then calibrated the CGMY parameters to these option prices. We see significant errors in pricing both SPX and VIX options based on the estimated parameters. While a poor performance is expected of a Lévy process as discussed in the first chapter, we do this calibration solely to benchmark the performance of our space scaled model. The joint estimation results of the space scaled model are provided in the next section.

4.4.2 Joint Calibration of SPX and VIX

Our purpose in implementing this model is to see how far a one-dimensional Markov model can go in pricing options on SPX and its expected future volatility, VIX. To see this, we calibrate our model to options on SPX and VIX simultaneously for all strikes and a single maturity on a given day. We follow Eberlein and Madan [25] by parametrizing the SPX option surface using the CGMY Self-Decomposable model. We then extract the vector of SPX option prices of all OTM strikes for the same maturities as the ones available in the VIX surface and optimize our model against these two option price vectors (SPX and VIX). See the Tables 4.2, 4.3, 4.4, 4.5, 4.6 below for the estimated parameters of our model. We also report the errors in terms of Average Percentage Errors (APEs), which is defined as the sum of absolute deviations of the model prices vs. the market prices divided by the sum of market prices. We use this metric since it places higher weights on errors in option prices near ATM strikes as compared to OTM strikes. One estimation was performed for each option maturity.

Since each day has options of multiple maturities, we perform the estimations for only five different days in our dataset. We chose the four days on which we got the best and worst APEs upon calibration to the SPX (11/21/07 and 10/09/07) and VIX option surfaces (11/20/07 and 09/27/07). These calibrations, which are described in greater detail in Sections 4.4.3 and 4.4.4, are separate calibrations of each surface (not to be confused with the joint calibration reported in this section). The fifth day (10/24/07) was chosen randomly from the dataset.

Date	*Mty*	S_0	G	M	Y	α	β	ξ	*errspx*	*errvix*
9/27/07	11/21/07	1,531	66.8	186.8	0.55	0.03	17.37	7.77	11.4%	3.5%
9/27/07	12/19/07	1,531	71.6	198.4	0.52	0.00	20.63	7.77	8.6%	8.7%
9/27/07	1/16/08	1,531	94.8	250.9	0.48	0.00	20.30	7.84	9.7%	6.1%
9/27/07	2/19/08	1,531	73.3	177.6	0.38	0.03	15.67	7.94	4.0%	2.9%
9/27/07	5/21/08	1,531	98.9	196.6	0.41	0.10	13.94	8.02	3.5%	5.7%

Table 4.2: This table shows the joint calibration results for the space scaled model (CGMYSSV) based on the market prices of options on 09/27/2007. We optimized the model separately for each option maturity. We chose five different dates from the dataset for our joint calibrations. Four of the five days were chosen based on the best and worst performances of the (separate) calibration of the VIX and SPX option surfaces in terms of the APEs. The fifth day was chosen randomly from our dataset. The estimation results of the separate VIX and SPX surface calibrations are given in the next section. This date had the worst performance in terms of the VIX surface calibration.

We observe that our model passes the test of joint calibration of the SPX and VIX options of a given maturity. The estimated parameters vary across maturities. This points to the need for a time dependency (i.e. a term structure) of parameters. This is a possible direction for future research. We provide one such formulation in terms of forward prices of options on stock forwards. That model can be seen as an extension of our model expressed in terms of forward prices. In that formulation, we will only need a term structure for the space centering parameter ξ. The details of

$Date$	Mty	S_0	G	M	Y	α	β	ξ	$errspx$	$errvix$
10/9/07	11/21/07	1,566	43.7	138.3	0.52	0.00	19.95	7.71	13.4%	6.6%
10/9/07	12/19/07	1,566	52.7	153.9	0.55	0.00	22.58	7.71	10.0%	9.1%
10/9/07	1/16/08	1,566	58.1	203.2	0.52	0.02	18.93	7.77	10.6%	6.2%
10/9/07	2/15/08	1,566	73.5	137.3	0.49	0.00	23.59	7.76	10.6%	9.4%
10/9/07	5/21/08	1,566	107.1	130.3	0.44	0.00	21.06	7.86	7.4%	12.0%

Table 4.3: This table shows the joint calibration results for the space scaled model (CGMYSSV) based on the market prices of options on 10/09/2007. We optimized the model separately for each option maturity. We chose five different dates from the dataset for our joint calibrations. Four of the five days were chosen based on the best and worst performances of the (separate) calibration of the VIX and SPX option surfaces in terms of the APEs. The fifth day was chosen randomly from our dataset. The estimation results of the separate VIX and SPX surface calibrations are given in the next section. This date had the worst performance in terms of the SPX surface calibration.

$Date$	Mty	S_0	G	M	Y	α	β	ξ	$errspx$	$errvix$
10/24/07	12/19/07	1,516	14.3	57.4	0.68	0.00	5.70	7.79	7.3%	2.0%
10/24/07	1/16/08	1,516	67.2	194.4	0.51	0.02	16.83	7.85	3.9%	1.4%
10/24/07	2/15/08	1,516	77.6	187.2	0.49	0.02	16.45	7.89	3.3%	1.9%
10/24/07	3/19/08	1,516	84.5	196.6	0.48	0.01	15.86	7.94	3.3%	2.9%
10/24/07	5/21/08	1,516	101.8	164.0	0.45	0.01	16.09	7.97	2.9%	5.0%

Table 4.4: This table shows the joint calibration results for the space scaled model (CGMYSSV) based on the market prices of options on 10/24/2007. We optimized the model separately for each option maturity. We chose five different dates from the dataset for our joint calibrations. Four of the five days were chosen based on the best and worst performances of the (separate) calibration of the VIX and SPX option surfaces in terms of the APEs. The fifth day was chosen randomly from our dataset. The estimation results of the separate VIX and SPX surface calibrations are given in the next section. This date was randomly chosen from our dataset.

Date	*Mty*	S_0	G	M	Y	α	β	ξ	*errspx*	*errvix*
11/20/07	2/19/08	1,439	74.5	150.2	0.48	0.01	17.84	7.87	5.4%	2.5%
11/20/07	3/19/08	1,439	74.4	139.8	0.45	0.00	17.95	7.88	3.0%	3.5%
11/20/07	5/21/08	1,439	74.3	125.2	0.30	0.14	20.62	7.94	4.2%	7.6%

Table 4.5: This table shows the joint calibration results for the space scaled model (CGMYSSV) based on the market prices of options on 11/20/2007. We optimized the model separately for each option maturity. We chose five different dates from the dataset for our joint calibrations. Four of the five days were chosen based on the best and worst performances of the (separate) calibration of the VIX and SPX option surfaces in terms of the APEs. The fifth day was chosen randomly from our dataset. The estimation results of the separate VIX and SPX surface calibrations are given in the next section. This date had the best performance in terms of the VIX surface calibration.

Date	*Mty*	S_0	G	M	Y	α	β	ξ	*errspx*	*errvix*
11/21/07	2/19/08	1,417	100.5	203.2	0.56	0.00	19.71	7.84	4.2%	3.1%
11/21/07	3/19/08	1,417	91.0	159.3	0.53	0.01	18.22	7.85	2.9%	3.8%
11/21/07	5/21/08	1,417	101.9	142.5	0.43	0.01	19.25	7.91	3.2%	6.9%

Table 4.6: This table shows the joint calibration results for the space scaled model (CGMYSSV) based on the market prices of options on 11/21/2007. We optimized the model separately for each option maturity. We chose five different dates from the dataset for our joint calibrations. Four of the five days were chosen based on the best and worst performances of the (separate) calibration of the VIX and SPX option surfaces in terms of the APEs. The fifth day was chosen randomly from our dataset. The estimation results of the separate VIX and SPX surface calibrations are given in the next section. This date had the best performance in terms of the SPX surface calibration.

that model are described in the conclusion and future research section.

4.4.3 Calibration of SPX surface

We also perform a calibration of the SPX surface across strikes and maturities. We report the optimized parameters in Tables 4.7, 4.8 and 4.9 below. We also report the Average Percentage Error (APE) in the last column of each table.

4.4.4 Calibration of VIX surface

We reported the optimized parameters of the VIX surface calibration in Tables 4.10, 4.11 and 4.12. The APE are given in the last column of the table. The VIX options are quoted as annualized volatility in percent. So we scale the VIX function by $\sqrt{12}$ and multiply it by 100 before determining the option payoffs. We also report a figure which shows what the SPX and VIX implied VIX function looks like for the randomly selected day (October 24, 2007).

4.4.5 SPX Distribution Properties implied by VIX and SPX Calibrations

Jump Activity

We look at the distribution of the Y parameter by SPX and VIX. As noted earlier, a value of $Y > 1$ implies that the process is of infinite variation where as $Y < 1$ implies finite variation. We observe that the VIX surface consistently implies a process of finite variation for most days. The SPX on the other hand implies that the stock price

$Date$	G	M	Y	α	β	ξ	APE
8/22/2007	0.1239	1.4442	1.3880	0.0289	0.1127	8.0765	7.11%
8/23/2007	0.1129	0.8623	1.3880	0.0068	0.1483	8.0516	6.87%
8/24/2007	0.1028	0.8405	1.3331	0.0065	0.1037	8.1803	7.36%
8/27/2007	0.1172	0.9604	1.3917	0.0161	0.1948	7.9292	6.86%
8/28/2007	0.1412	1.2384	1.4316	0.0070	0.2090	7.9829	6.32%
8/29/2007	0.1242	0.9849	1.3935	0.0057	0.1817	8.0129	6.72%
8/30/2007	0.1307	1.0727	1.4122	0.0055	0.1953	8.0029	6.58%
8/31/2007	0.1225	0.9909	1.4043	0.0069	0.1705	8.0355	6.98%
9/4/2007	0.1177	1.0241	1.3963	0.0054	0.1604	8.0612	7.45%
9/5/2007	0.1328	1.3185	1.4463	0.0086	0.1950	8.0089	7.35%
9/6/2007	0.1288	1.2545	1.4272	0.0077	0.1782	8.0398	7.46%
9/7/2007	0.1458	1.4724	1.4508	0.0098	0.2237	7.9820	7.02%
9/10/2007	0.1506	1.4863	1.4632	0.0107	0.2392	7.9647	6.95%
9/11/2007	0.1373	1.3807	1.4473	0.0064	0.2018	8.0185	7.37%
9/12/2007	0.1361	1.3414	1.4455	0.0092	0.1996	8.0103	7.25%
9/13/2007	0.1342	1.2892	1.4400	0.0126	0.2124	7.9761	7.17%
9/14/2007	0.1339	1.2744	1.4379	0.0078	0.2096	7.9965	7.23%
9/17/2007	0.1418	1.3348	1.4601	0.0146	0.2455	7.9353	7.18%
9/18/2007	0.1063	0.8235	1.3312	0.0088	0.1204	8.1430	7.76%
9/19/2007	0.0712	5.5340	1.2801	0.0022	0.8920	7.7901	7.02%
9/20/2007	0.0425	130.5821	0.9879	0.1160	5.9125	7.8413	6.63%
9/21/2007	0.0390	88.5232	0.9677	0.0011	3.6070	7.9443	6.66%
9/24/2007	0.0477	50.5986	1.0293	0.0140	2.1153	7.9544	6.34%
9/25/2007	0.0475	41.2045	1.0290	0.0040	1.6527	7.9945	6.13%
9/26/2007	0.0467	24.5190	1.0263	0.0634	0.8710	8.0721	6.39%

Table 4.7: This table shows the parameters of the space scaled model (CGMYSSV) calibrated to the SPX options surface (option prices across different strikes and maturities). We did not use any VIX option prices for this calibration. The model was calibrated to all OTM SPX options with maturities between one month and one year. One calibration was performed for each day. We also report the Average Percentage Error (APE) of the option prices based on the estimated parameters. We see a reasonable fit of our model to the SPX surface. We note that this is a significant improvement over Lévy process based models as they do not calibrate well to the surface of option prices across different maturities and strikes.

Date	G	M	Y	α	β	ξ	APE
9/27/2007	0.0442	22.7379	1.0343	0.0003	0.9349	8.0759	6.44%
9/28/2007	0.0431	31.4266	1.0273	0.0016	1.2988	8.0353	6.43%
10/1/2007	0.0438	35.8966	1.0131	0.0010	1.2780	8.0730	6.66%
10/2/2007	0.0445	35.0020	1.0135	0.0001	1.3148	8.0716	6.10%
10/3/2007	0.0449	46.9780	0.9934	0.0004	1.6658	8.0619	5.98%
10/4/2007	0.0899	0.5652	1.2533	0.0088	0.0889	8.2209	7.18%
10/5/2007	0.0808	0.4570	1.2233	0.0180	0.1091	8.0426	8.25%
10/8/2007	0.0831	0.5121	1.2358	0.0146	0.0854	8.1739	8.09%
10/9/2007	0.0764	0.4013	1.2091	0.0221	0.1062	8.0022	8.93%
10/10/2007	0.0818	0.4493	1.2233	0.0169	0.0945	8.1039	8.48%
10/12/2007	0.0875	0.4485	1.2263	0.0001	0.0897	8.2642	8.06%
10/15/2007	0.0984	0.6220	1.2700	0.0148	0.1047	8.1625	6.71%
10/16/2007	0.1046	0.7471	1.3008	0.0125	0.0969	8.2357	6.23%
10/17/2007	0.0951	0.5588	1.2391	0.0070	0.0971	8.2254	5.91%
10/18/2007	0.0565	14.6725	1.0309	0.0622	0.5659	8.1568	5.05%
10/19/2007	0.0457	181.3094	0.9102	0.0183	4.4411	8.0894	4.48%
10/22/2007	0.0454	126.9806	0.9210	0.0000	4.2219	8.0208	4.75%
10/23/2007	0.0546	37.6734	0.9796	0.0031	1.3405	8.1133	5.15%
10/24/2007	0.0676	14.2210	1.0821	0.0042	0.8536	8.0231	5.05%
10/25/2007	0.0579	48.1957	0.9989	0.0024	1.9166	8.0326	5.25%
10/26/2007	0.0608	14.6591	1.0214	0.0086	0.6781	8.1437	5.93%
10/29/2007	0.0632	11.1187	1.0572	0.0056	0.6691	8.0817	6.07%
10/30/2007	0.0636	18.3149	1.0495	0.0020	1.0429	8.0355	5.56%
10/31/2007	0.0549	8.6767	0.9984	0.0055	0.5187	8.1572	7.14%
11/1/2007	0.0577	95.1224	0.9746	0.0000	3.9010	7.9631	5.12%

Table 4.8: This table shows the parameters of the space scaled model (CGMYSSV) calibrated to the SPX options surface (option prices across different strikes and maturities). We did not use any VIX option prices for this calibration. The model was calibrated to all OTM SPX options with maturities between one month and one year. One calibration was performed for each day. We also report the Average Percentage Error (APE) of the option prices based on the estimated parameters. We see a reasonable fit of our model to the SPX surface. We note that this is a significant improvement over Lévy process based models as they do not calibrate well to the surface of option prices across different maturities and strikes.

Date	G	M	Y	α	β	ξ	APE
11/2/2007	0.0578	94.7307	0.9723	0.0000	3.9224	7.9636	5.23%
11/5/2007	0.0908	8.0512	1.2465	0.0016	1.1774	7.8019	5.48%
11/6/2007	0.0610	73.5668	0.9558	0.2539	2.4647	7.9876	5.58%
11/7/2007	0.1161	1.3354	1.2108	0.0608	0.3257	7.7337	6.29%
11/8/2007	0.1176	1.6215	1.2057	0.0680	0.4131	7.6760	6.18%
11/9/2007	0.1421	3.4072	1.3168	0.0833	0.6155	7.6249	5.13%
11/12/2007	0.1450	3.1253	1.2527	0.0935	0.6163	7.5745	6.68%
11/13/2007	0.0684	71.2021	0.9840	0.0107	3.0411	7.9541	5.37%
11/14/2007	0.1167	1.5639	1.2604	0.0789	0.7234	7.5564	6.22%
11/15/2007	0.1371	2.1191	1.3020	0.0677	0.5056	7.6750	5.37%
11/16/2007	0.0825	60.6879	1.0289	0.0000	3.5263	7.8594	5.37%
11/19/2007	0.1245	2.2720	1.2395	0.0725	0.5980	7.6429	5.91%
11/20/2007	0.0830	38.4240	1.0807	0.0000	2.8266	7.8343	5.24%
11/21/2007	0.0675	98.9019	0.9929	0.0000	5.3142	7.8631	4.38%
11/22/2007	0.1197	2.9551	1.3223	0.0722	0.9129	7.6087	5.07%
11/23/2007	0.0717	54.3701	1.0340	0.0000	3.2975	7.8794	4.43%
11/26/2007	0.1436	2.2793	1.2777	0.0959	0.4512	7.6080	6.07%
11/27/2007	0.0647	87.5431	1.0080	0.0009	4.7795	7.8736	4.51%
11/28/2007	0.0608	43.7528	0.9996	0.0000	2.4932	7.9613	5.41%
11/29/2007	0.0581	51.8948	0.9802	0.0001	2.9906	7.9495	5.30%

Table 4.9: This table shows the parameters of the space scaled model (CGMYSSV) calibrated to the SPX options surface (option prices across different strikes and maturities). We did not use any VIX option prices for this calibration. The model was calibrated to all OTM SPX options with maturities between one month and one year. One calibration was performed for each day. We also report the Average Percentage Error (APE) of the option prices based on the estimated parameters. We see a reasonable fit of our model to the SPX surface. We note that this is a significant improvement over Lévy process based models as they do not calibrate well to the surface of option prices across different maturities and strikes.

Date	G	M	Y	α	β	ξ	*APE*
8/22/2007	0.0176	0.0315	0.2490	0.0001	0.0296	7.7237	4.41%
8/23/2007	0.0224	0.0405	0.2834	0.0000	0.0405	7.7202	5.58%
8/24/2007	0.0151	0.0256	0.2454	0.0001	0.0256	7.7241	4.55%
8/27/2007	0.0310	0.0633	0.2910	0.0004	0.0603	7.6979	5.17%
8/28/2007	0.1042	0.4559	0.7559	0.0000	0.4546	7.6354	7.18%
8/29/2007	0.0295	0.0568	0.3165	0.0001	0.0558	7.7234	5.67%
8/30/2007	0.0156	0.0399	0.2436	0.0001	0.0391	7.6715	5.87%
8/31/2007	0.0416	0.0738	0.2976	0.0008	0.0738	7.7029	4.29%
9/4/2007	0.0195	0.0380	0.2556	0.0001	0.0362	7.7268	3.82%
9/5/2007	0.0210	0.0474	0.2654	0.0001	0.0465	7.6942	5.02%
9/6/2007	0.0011	0.0024	0.1356	0.0000	0.0024	7.6785	4.99%
9/7/2007	0.0040	0.0125	0.1695	0.0000	0.0110	7.6555	6.09%
9/10/2007	0.0301	0.0289	0.2472	0.0016	0.0288	7.7753	7.02%
9/11/2007	0.0117	0.0324	0.2326	0.0000	0.0317	7.6739	5.77%
9/12/2007	0.0307	0.0925	0.3320	0.0001	0.0906	7.6752	5.89%
9/13/2007	0.0289	0.0959	0.3274	0.0008	0.0958	7.6521	5.58%
9/14/2007	0.0255	0.0765	0.3265	0.0001	0.0760	7.6830	5.74%
9/17/2007	0.0405	0.0403	0.3386	0.0003	0.0401	7.8609	6.73%
9/18/2007	0.0354	0.0640	0.3952	0.0001	0.0633	7.7762	2.86%
9/19/2007	0.0842	0.1606	0.6432	0.0008	0.1606	7.7886	2.21%
9/20/2007	0.0724	0.1648	0.6224	0.0004	0.1643	7.7651	2.37%
9/21/2007	0.0504	0.1037	0.4314	0.0000	0.0902	7.7775	2.89%
9/24/2007	0.0198	0.0334	0.3186	0.0003	0.0332	7.7578	2.14%
9/25/2007	0.0842	0.1724	0.6533	0.0014	0.1723	7.7633	2.37%
9/26/2007	0.3123	0.1812	0.5678	0.0000	0.1666	7.8456	5.31%

Table 4.10: This table shows the parameters of the space scaled model (CGMYSSV) calibrated to the VIX options surface (option prices across different strikes and maturities). We did not use any SPX option prices for this calibration. The model was calibrated to all ITM VIX options with maturities between one month and one year. Since OTM options are more liquid, we used the ITM option prices implied by OTM options using put-call parity. One calibration was performed for each day. We also report the Average Percentage Error (APE) of the option prices based on the estimated parameters. We see a very good fit of our model to the VIX surface. We note that this is a significant improvement over Lévy process which cannot price options on VIX as they assume that volatility is completely deterministic.

Date	G	M	Y	α	β	ξ	APE
9/27/2007	0.0014	0.0013	0.1436	0.0000	0.0013	7.7870	8.75%
9/28/2007	0.0303	0.0611	0.3633	0.0011	0.0607	7.7276	2.54%
10/1/2007	0.0973	0.1363	0.6024	0.0005	0.1362	7.8166	2.19%
10/2/2007	0.0979	0.1949	0.7251	0.0006	0.1931	7.7967	2.19%
10/3/2007	0.0897	0.1241	0.3097	0.0002	0.0922	7.8175	2.29%
10/4/2007	0.0397	0.0512	0.3138	0.0001	0.0508	7.7902	2.89%
10/5/2007	0.5213	0.5177	1.0224	0.0009	0.3726	7.8137	3.54%
10/8/2007	0.1131	0.0640	0.2888	0.0001	0.0639	7.8223	5.91%
10/9/2007	0.0308	0.0552	0.3219	0.0001	0.0548	7.7306	4.80%
10/10/2007	0.1816	0.4688	1.1238	0.0001	0.3808	7.7579	3.22%
10/12/2007	0.0807	0.0995	0.3043	0.0012	0.0908	7.7828	2.79%
10/15/2007	0.1648	0.3037	0.8284	0.0000	0.2872	7.8060	2.37%
10/16/2007	0.0492	0.0780	0.3266	0.0003	0.0776	7.7681	2.62%
10/17/2007	0.0686	0.1052	0.3472	0.0017	0.1052	7.7534	2.58%
10/18/2007	0.2364	0.4341	1.1348	0.0000	0.4341	7.7437	4.17%
10/19/2007	0.0290	0.0589	0.3175	0.0001	0.0584	7.7370	3.17%
10/22/2007	0.0183	0.0296	0.2971	0.0003	0.0295	7.7672	2.50%
10/23/2007	0.0250	0.0424	0.3318	0.0004	0.0421	7.7716	2.29%
10/24/2007	0.0434	0.0864	0.4147	0.0001	0.0826	7.7745	2.37%
10/25/2007	0.0373	0.0736	0.4053	0.0002	0.0732	7.7687	2.44%
10/26/2007	0.0266	0.0397	0.2977	0.0007	0.0396	7.7669	2.41%
10/29/2007	0.0370	0.0517	0.3099	0.0011	0.0516	7.7682	2.45%
10/30/2007	0.0270	0.0476	0.3098	0.0006	0.0475	7.7601	2.62%
10/31/2007	0.0390	0.0410	0.2948	0.0005	0.0410	7.8062	2.77%
11/1/2007	0.0199	0.0411	0.3028	0.0002	0.0410	7.7446	2.84%

Table 4.11: This table shows the parameters of the space scaled model (CGMYSSV) calibrated to the VIX options surface (option prices across different strikes and maturities). We did not use any SPX option prices for this calibration. The model was calibrated to all ITM VIX options with maturities between one month and one year. Since OTM options are more liquid, we used the ITM option prices implied by OTM options using put-call parity. One calibration was performed for each day. We also report the Average Percentage Error (APE) of the option prices based on the estimated parameters. We see a very good fit of our model to the VIX surface. We note that this is a significant improvement over Lévy process which cannot price options on VIX as they assume that volatility is completely deterministic.

$Date$	G	M	Y	α	β	ξ	APE
11/2/2007	0.0350	0.0689	0.3458	0.0004	0.0687	7.7583	2.78%
11/5/2007	0.0286	0.0527	0.3037	0.0007	0.0526	7.7470	2.64%
11/6/2007	0.0323	0.0520	0.3332	0.0001	0.0514	7.7902	3.01%
11/7/2007	0.0277	0.0646	0.2964	0.0002	0.0609	7.7321	2.91%
11/8/2007	0.0494	0.1102	0.3896	0.0002	0.1095	7.7334	2.89%
11/9/2007	0.0215	0.0521	0.2753	0.0001	0.0519	7.7008	2.87%
11/12/2007	2.9447	2.6073	0.8180	0.0000	0.8217	7.9684	6.88%
11/13/2007	0.4688	1.7173	0.7765	0.0000	0.5977	7.8047	2.41%
11/14/2007	0.0257	0.0710	0.2978	0.0002	0.0705	7.6925	2.63%
11/15/2007	0.0856	0.3561	0.6127	0.0001	0.3531	7.6702	2.54%
11/16/2007	0.1469	0.4909	0.8032	0.0014	0.4247	7.7226	2.27%
11/19/2007	0.0530	0.1481	0.3259	0.0032	0.1479	7.6355	1.96%
11/20/2007	0.0347	0.0721	0.3302	0.0001	0.0716	7.7297	1.79%
11/21/2007	0.0603	0.1240	0.3869	0.0001	0.1239	7.7124	2.03%
11/22/2007	0.0713	0.1478	0.4205	0.0002	0.1475	7.7128	2.00%
11/23/2007	0.0848	0.1911	0.4345	0.0000	0.1712	7.7338	2.12%
11/26/2007	0.0359	0.0741	0.3291	0.0000	0.0702	7.7174	2.51%
11/27/2007	0.0245	0.0503	0.2944	0.0001	0.0496	7.7215	2.78%
11/28/2007	0.7417	2.9898	0.6595	0.0174	0.7664	7.7859	2.31%
11/29/2007	0.0870	0.2063	0.4916	0.0000	0.1768	7.7572	2.63%

Table 4.12: This table shows the parameters of the space scaled model (CGMYSSV) calibrated to the VIX options surface (option prices across different strikes and maturities). We did not use any SPX option prices for this calibration. The model was calibrated to all ITM VIX options with maturities between one month and one year. Since OTM options are more liquid, we used the ITM option prices implied by OTM options using put-call parity. One calibration was performed for each day. We also report the Average Percentage Error (APE) of the option prices based on the estimated parameters. We see a very good fit of our model to the VIX surface. We note that this is a significant improvement over Lévy process which cannot price options on VIX as they assume that volatility is completely deterministic.

process is of infinite activity. Thus VIX implied SPX distribution underestimates the amount of small jump activity of the underlying index. This may be explained by the fact that since VIX measures the expectations of square returns, the process of squaring returns underweighs small jumps activity versus the large jumps of the underlying SPX index.

Skewness

While we are unable to calculate the skewness in closed form, we use a proxy to qualitatively measure the skewness of the underlying index. We observe that the parameters G and M exponentially dampen the amount of negative and positive jump activity. Thus if $G < M$, the model would imply greater dampening of positive jumps, or negative skewness. On the other hand, $G > M$ implies a positive skewness and $G = M$ implies a symmetric return distribution. We, therefore, use $G - M$ as a proxy for skewness. Based on this measure, we note that the SPX index implies very high levels of skewness whereas skewness of the VIX implied SPX distribution is close to symmetric. This is again not surprising since volatility does not distinguish between positive or negative jumps.

We observe that the VIX index as a function of SPX level implied by the two option surfaces is very different. We plot the implied VIX index from the two surface calibrations for each of the five days.

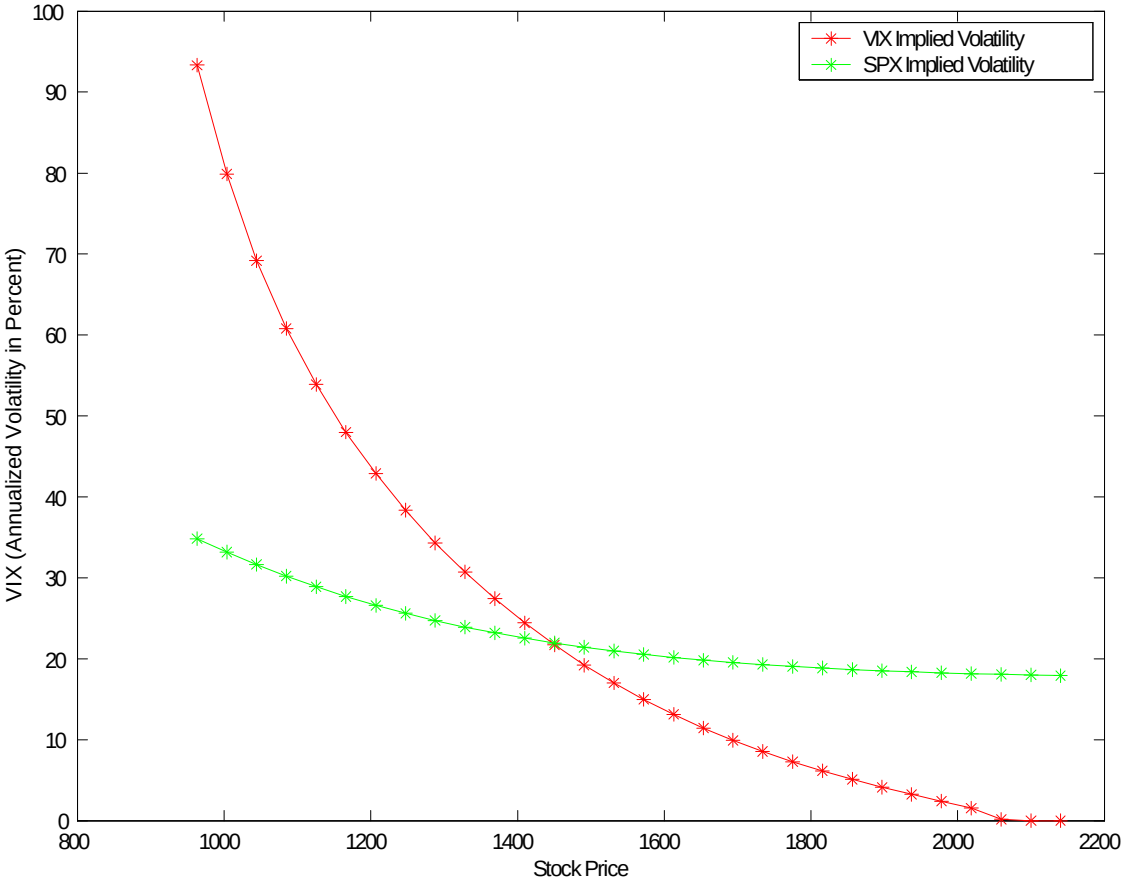

Figure 4-1: This graph shows the model implied VIX as a function of the S&P500 levels as of 9/27/2007. The VIX function is estimated from the model (see equations (1.8) and (1.2)). The parameters are based on the calibration to SPX option prices (green graph) and the VIX option prices (red graph). We chose 9/27/2007 as this was the day of the worst VIX calibration performance in terms of APEs.

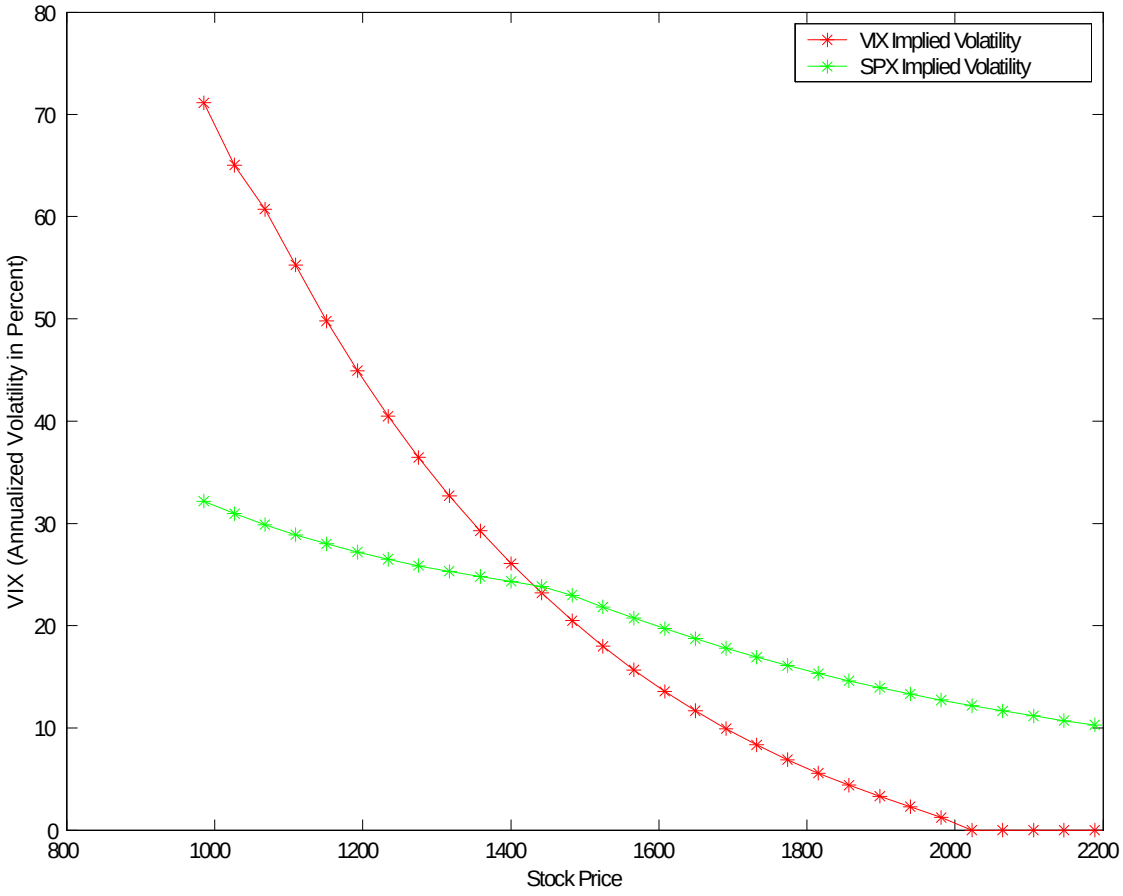

Figure 4-2: This graph shows the model implied VIX as a function of the S&P500 levels as of 10/9/2007. The VIX function is estimated from the model (see equations (1.8) and (1.2)). The parameters are based on the calibration to SPX option prices (green graph) and the VIX option prices (red graph). We chose 10/9/2007 as this was the day of the worst SPX calibration performance in terms of APEs.

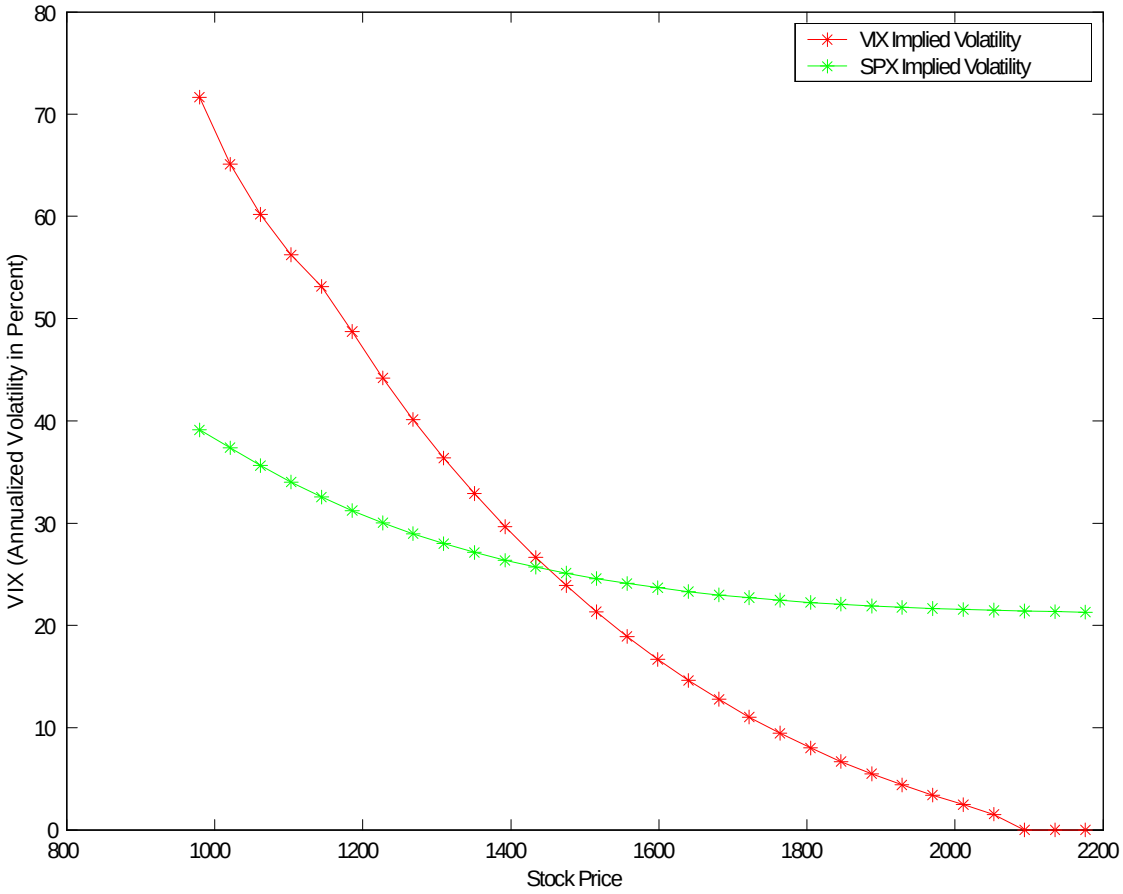

Figure 4-3: This graph shows the model implied VIX as a function of the S&P500 levels as of 10/24/2007. The VIX function is estimated from the model (see equations (1.8) and (1.2)). The parameters are based on the calibration to SPX option prices (green graph) and the VIX option prices (red graph). We chose 10/24/2007 as a randomly selected day from our dataset. Four other days were chosen based on the worst and best performances of the calibration to the SPX and VIX surfaces.

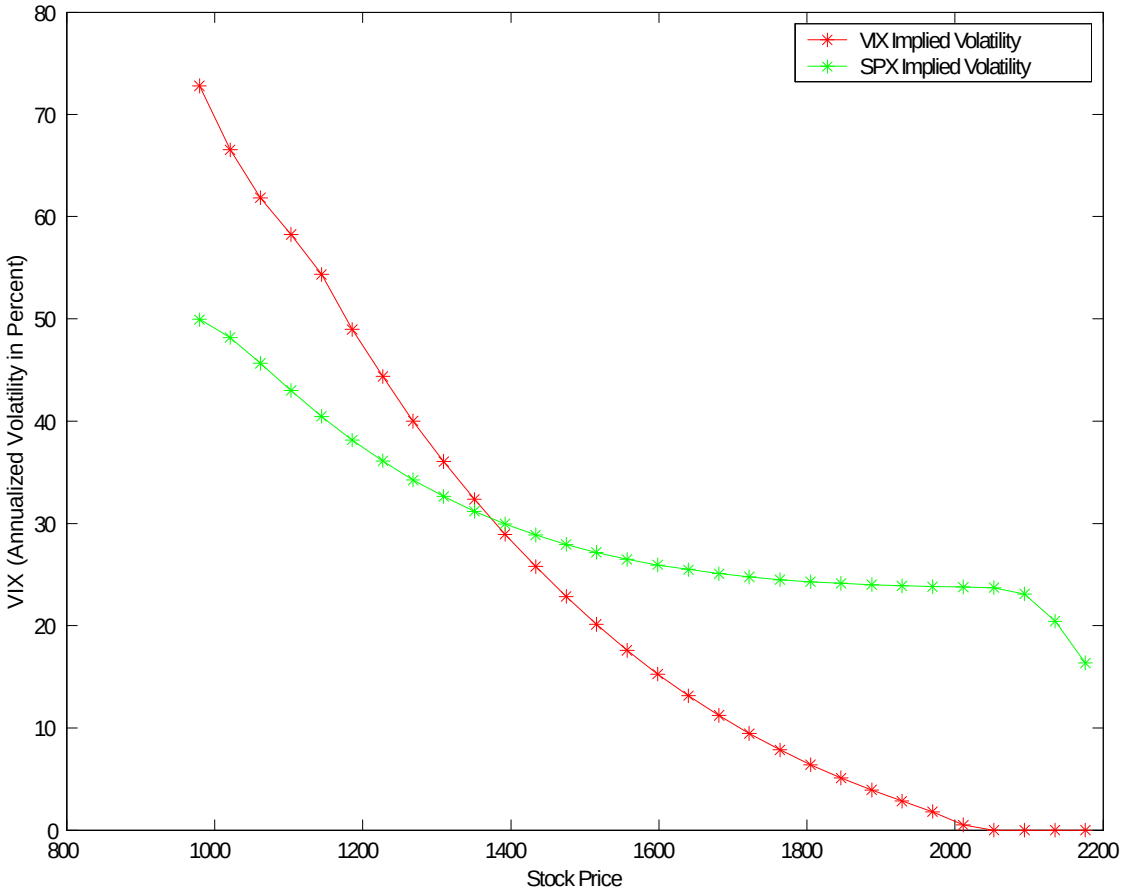

Figure 4-4: This graph shows the model implied VIX as a function of the S&P500 levels as of 11/20/2007. The VIX function is estimated from the model (see equations (1.8) and (1.2)). The parameters are based on the calibration to SPX option prices (green graph) and the VIX option prices (red graph). We chose 11/20/2007 as this was the day of the best VIX calibration performance in terms of APEs.

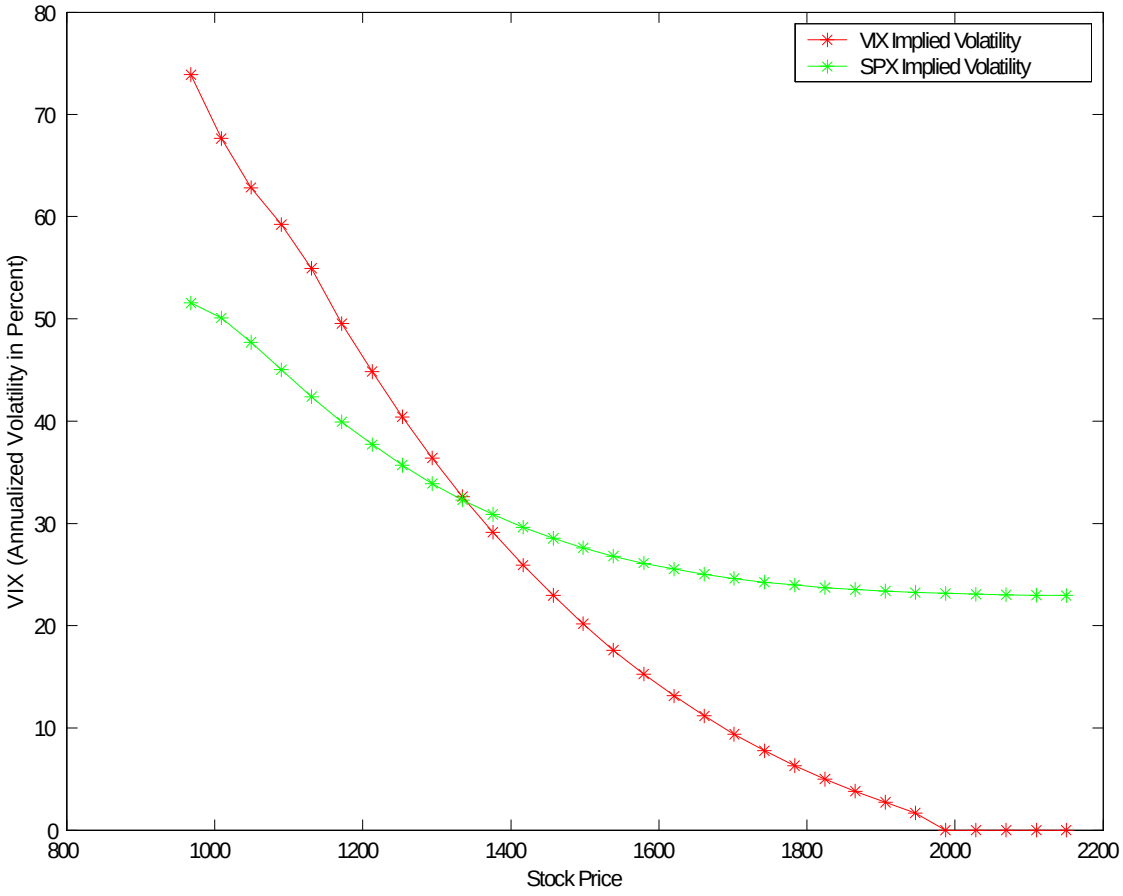

Figure 4-5: This graph shows the model implied VIX as a function of the S&P500 levels as of 11/21/2007. The VIX function is estimated from the model (see equations (1.8) and (1.2)). The parameters are based on the calibration to SPX option prices (green graph) and the VIX option prices (red graph). We chose 11/21/2007 as this was the day of the best SPX calibration performance in terms of APEs.

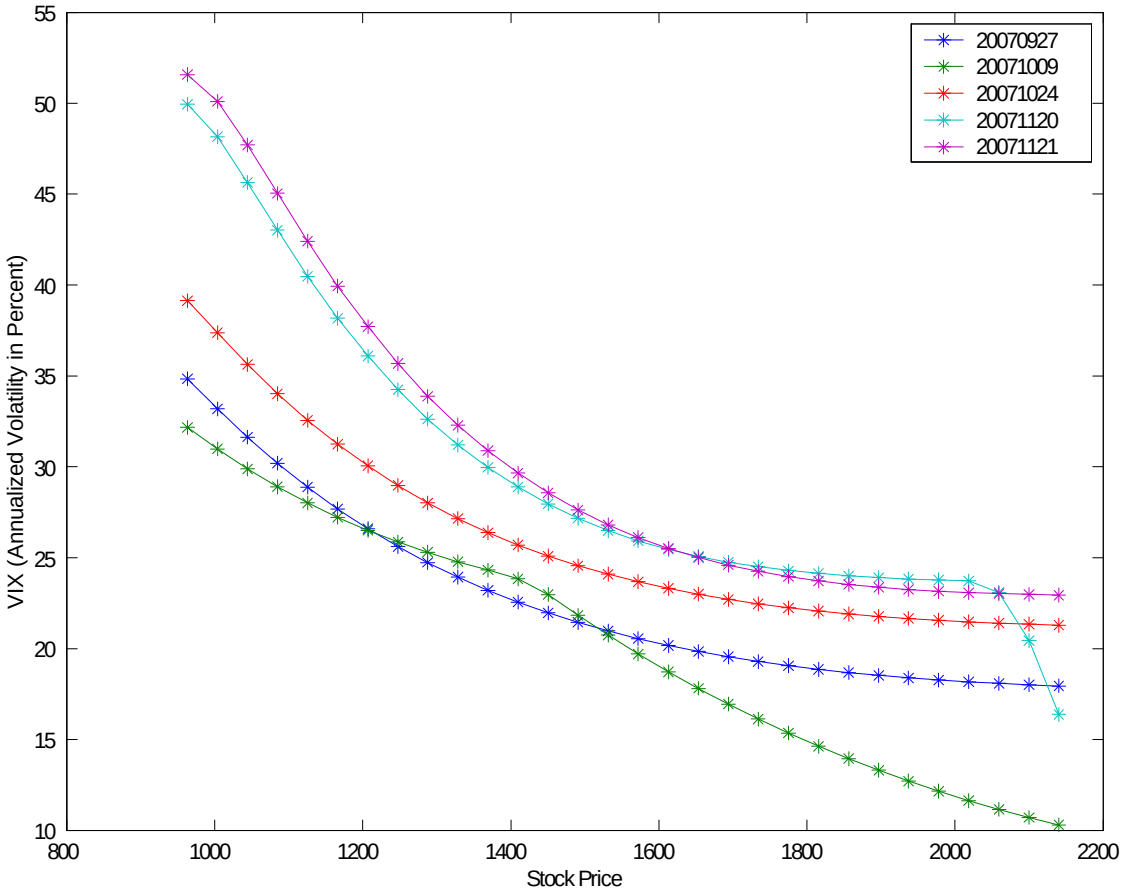

Figure 4-6: This graph shows the VIX function as implied by the model based on SPX option prices for five different days . For each of these five days, we calibrate our model to the SPX option price surface. We plot the implied VIX function (see equations (1.8) and (1.2)) based on the calibrated parameters. The details of the calibration are in Section 4.4.3. Four of the five days were chosen based on the best and worst performances of the calibration of the VIX and SPX option surfaces in terms of the APEs. The fifth day was chosen randomly from our dataset. We see that the VIX function implied by SPX option is different across different days. This period (August to November, 2007) was when the VIX index became prominent after the start of the sub-prime crisis. When compared with the following graph which shows the VIX function as implied by VIX options, one sees that the SPX options do not provide a stable estimate of the VIX function across different days.

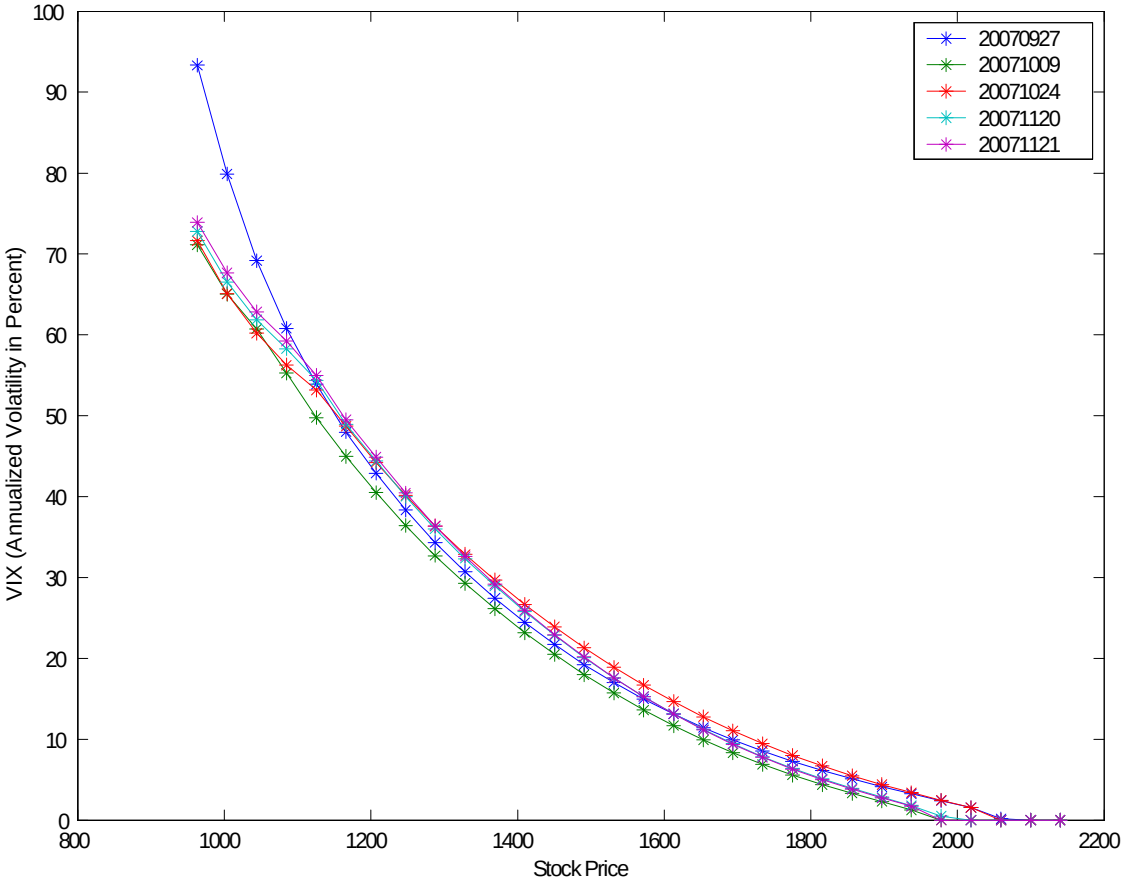

Figure 4-7: This graph shows the VIX function as implied by the model based on VIX option surface for five different days. For each of those five days, we calibrate our model to the VIX option price surface. We plot the implied VIX function (see equations (1.8) and (1.2)) based on the calibrated parameters. The details of the calibration are in Section 4.4.4. Four of the five days were chosen based on the best and worst performances of the calibration of the VIX and SPX option surfaces in terms of the APEs. The fifth day was chosen randomly from our dataset. We see that the VIX function implied by the VIX options' based parameters is fairly stable across different days as compared to the VIX function implied by the SPX options in the previous graph.

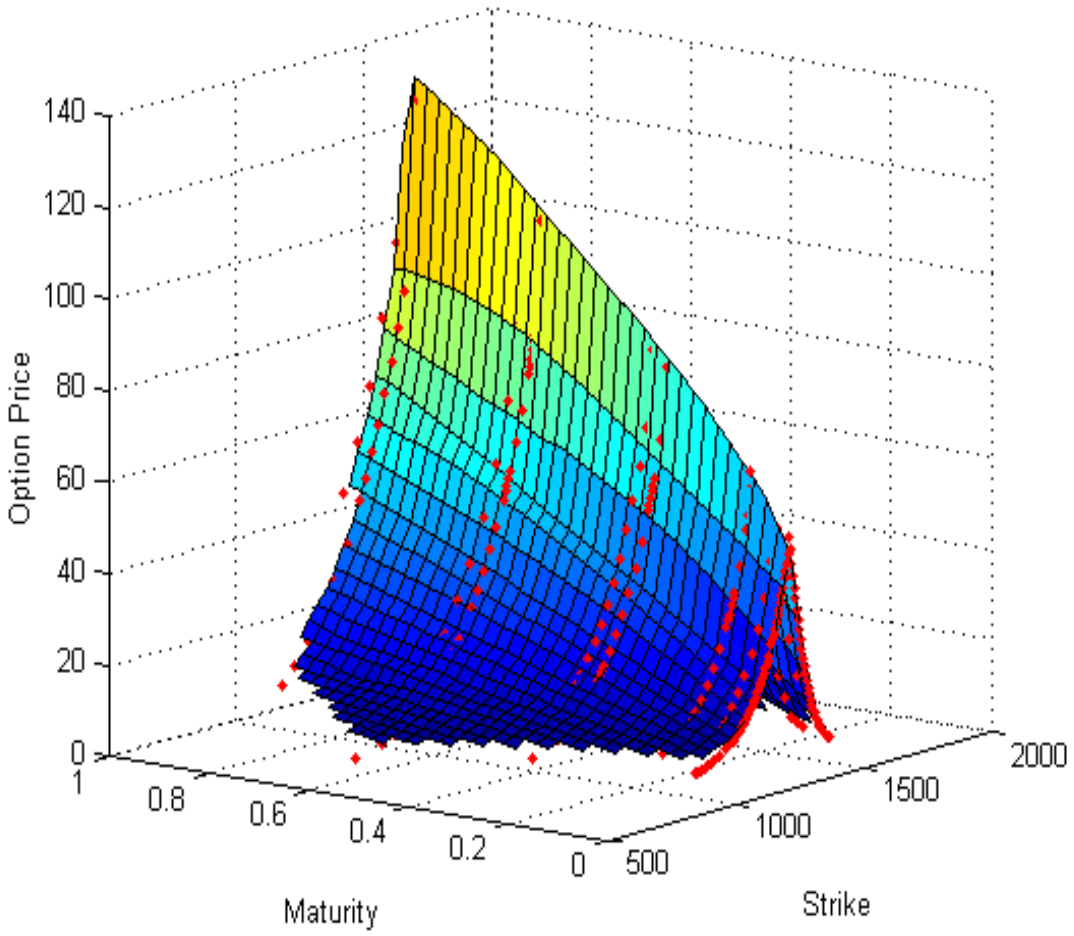

Figure 4-8: This graph gives the SPX OTM option prices on 10/24/2007. The horizontal axes represent the option strikes in terms of SPX levels and maturities in years. The strikes lower (higher) than around 1516 represent put (call) options. The red dots represent market prices and the surface represents the model prices based on the calibrated parameters.

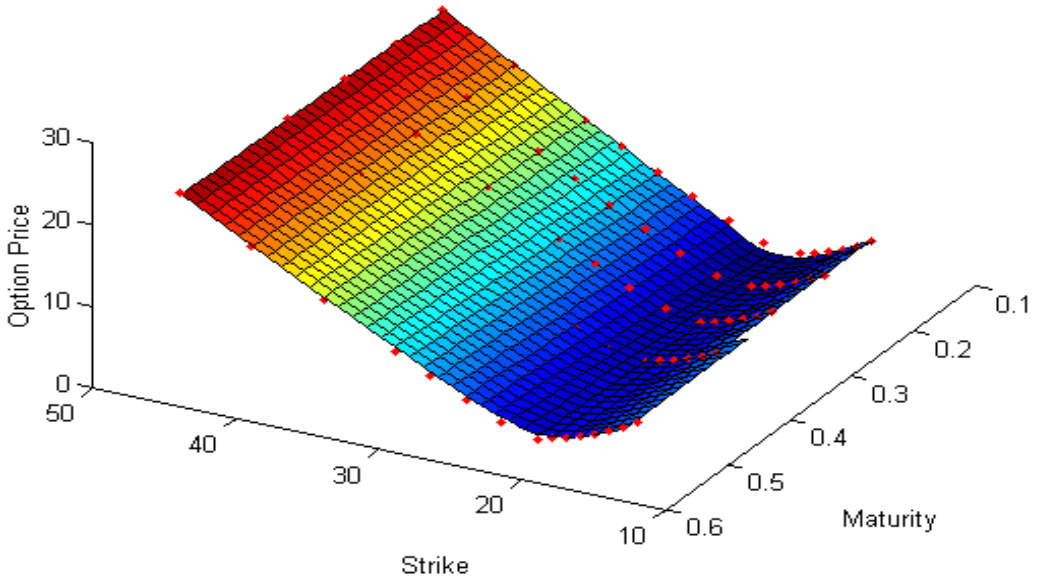

Figure 4-9: This graph gives the VIX ITM option prices on 10/24/2007. The horizontal axes represent the option strikes (volatilities) and maturities.The strike prices are given as annualized volatilities in percentage terms. The option maturities are given in years. The strikes lower (higher) than around 20 (percent) represent call (put) options. The red dots represent market prices and the surface represents the model prices based on the calibrated parameters.

Chapter 5

Conclusion and Future research

5.1 Conclusion

Our model is the first attempt to generalize a Lévy processes to create a space-dependent pure jump process. We achieve this in a one-dimensional Markov setting using six degrees of freedom. Our model successfully calibrates option prices on SPX and VIX indices simultaneously for any given maturity. Our model is also able to capture the SPX and VIX surfaces separately. This is a huge improvement over Lévy processes which implicitly assume a deterministic volatility (VIX) function. We estimate our model on the SPX and VIX option surfaces as well and note that the model calibrates well to both these surfaces separately. We explored the properties of the implied distribution of the SPX from both indices and conclude that the VIX index under-weighs small jumps as compared to large jumps as well as skewness of the SPX index . We also devised a multi-stage scheme to numerically calculate the VIX function as a function of the underlying stock price since no closed form was

available.

We also note that since our model can price both SPX and VIX options simultaneously, it will show no-arbitrage prices for the variance swap contract. This is because the VIX option prices are computed directly from the price of the log contract using equation (1.8). Hence a portfolio of VIX options will return the same price for the log contract. Since we use the same (jointly calibrated) parameters for pricing the SPX options, the SPX options will also return the same price for the log contract. This will ensure a no-arbitrage price of the variance swap as both replication schemes will price the variance swap contract through equation (1.8).

5.2 Numerical Computation Using Wavelets

While the results of our model are quite satisfactory, a lot more can be done to improve the computational efficiency of our model. If one needs to work with more than 40-50 grid points, it would be better to implement the solution using a wavelet basis, on the lines of Matache, von Petersdorff, Schwab [41] and. They have shown that for the Lévy process, one can reduce the number of non-zero entries in the stiffness matrix from $O(N^2)$ to $O(N \log N^\beta)$ for some $\beta > 0$. Matache, von Petersdorff, Schwab [41] show that their results can be applied to space-dependent processes as well. One can further improve the efficiency of the numerical solution by using iterative methods for solving the linear system of equations and also by using higher order time stepping schemes (see Matache, Schwab, Wihler [40] for implementation of this idea in the context of Lévy processes).

5.3 Skewness and Kurtosis Properties

It has been observed in Madan [37] that creating stochastic volatility through time scaling leads to an inverse relationship between skewness and volatility whereas space scaling leads to a direct relationship between the two. The market data also implies a direct relationship between volatility and skewness. One future area of research is to perform mode detailed analysis of the nature of this relationship in our model setting.

5.4 Model Extensions

5.4.1 Model Formulation in Forward Space

One can further generalize our model by introducing time dependence along with space-dependence. This would be the next logical step towards creating a local Lévy model. We provide one natural extension of our model in forward space. We start with the PIDE for option prices for space-scaled Lévy processes given in (3.7)

$$w_\tau(\tau, x) + Aw(\tau, x) = 0, \tag{5.1}$$

$$Aw(\tau, x) = -(r - q)w_x(\tau, x) + rw(\tau, x) + \hat{A}w(\tau, x), \text{ where}$$

$$\hat{A}w(\tau, x) = -\int_{-\infty}^{\infty} \left(w(\tau, x + z) - w(\tau, x) - w_x(\tau, x)(e^z - 1)\right) k(z, x)dz;$$

$$w(0, x) = h(x).$$

We transform this equation to solve for forward option prices in terms of forwards on the underlying, that is, if we let $u(y)=e^{r\tau}w(x)$, with $y = x + (r-q)\tau$, we transform the equation into

$$u_\tau(\tau, y) + \tilde{A}u(\tau, y) = 0, \tag{5.2}$$

$$\tilde{A}u(\tau, y) = -\int_{-\infty}^{\infty} \left(u(\tau, y+z) - u(\tau, y) - u_y(\tau, y)(e^z - 1)\right) k(z, y-(r-q)\tau)dz;$$

$$u(0, y) = \tilde{h}(y).$$

By the definition of our space scaled density function for the CGMY process, we have for $z > 0$

$$\begin{aligned} k(z, y-(r-q)\tau) &= a(y-(r-q)\tau)^Y e^{-Mz/a(y-(r-q)\tau)} z^{-1-Y}, \\ a(y-(r-q)\tau) &= \alpha + \beta(y-(r-q)\tau-\xi)^2 \\ &= \alpha + \beta(y-\xi_\tau)^2, \text{ where} \\ \xi_\tau &= (r-q)\tau + \xi \end{aligned}$$

Thus we see that our model has a natural generalization in terms of forward prices through a term structure of ξ_τ, while keeping α and β constant. This would put the new model in a parametric space-time local volatility framework. We currently have only space dependence in our local volatility model. Such a model would impose numerical challenges in computing a different stiffness matrix for each time step. One way to overcome such an issue would be to employ a parallel computing framework since the same stiffness matrix will be used for all options of the same maturity.

5.4.2 The Need for Stochastic Volatility

While our model tries to stay in the one dimensional Markovian framework, a pertinent question that still needs to be answered is whether the VIX index prices in the stochasticity of volatility. After all, it can be argued that the solution of the log contract follows equation (1.11), which makes VIX a function of time, stock level and stochastic volatility. Indeed, if VIX was a deterministic function of the SPX index, it would imply that no price discovery takes place in the VIX market, thus eliminating the very reason for its existence. On the other hand, stochastic volatility models which don't take into account the space dependence are unable to capture the leverage effect. Thus, they will most likely be inaccurate in determining the hidden volatility process as the effect of leverage cannot be filtered out before determining the innovation coming from the second hidden dimension. We also observe that the market implied leverage function for VIX and SPX calibrations are not very different. We test this by freezing the G, M, Y parameters and calibrating the α, β and ξ parameters to the SPX and VIX surface. We plot the leverage function for the randomly selected day (10/24/2007). We observe that VIX options imply a higher leverage than SPX options (see Figure 5-1).

5.4.3 Time Dependence

It is reasonable to assume that the leverage effect decays in time; volatility subsides over time as the stock moves to a new level and the leverage gets priced in. A distinct time component would be necessary to model this effect. However, time dependence

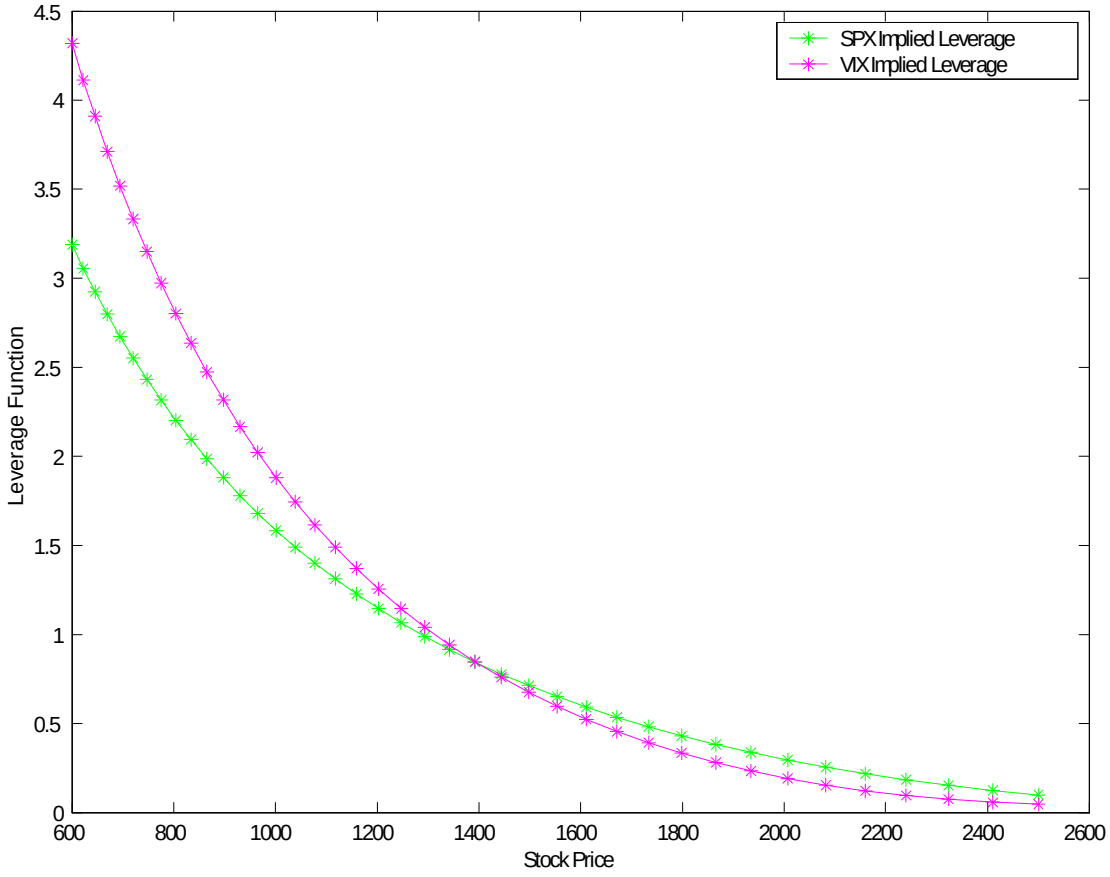

Figure 5-1: Leverage function plots based on SPX and VIX calibration of α, β and ξ parameters while setting $G = 5, M = 10$ and $Y = .75$. The option surfaces are as of 10/24/2007.

will mean that our jump operator is no longer time-invariant. This would mean that the PIDE from such a process would involve a different operator in each-time step. Implementing such a model by brute force may be inefficient as a new stiffness matrix will need to be calculated for each time step. However, the problem may be resolved by using a parallel-computing framework or the wavelet methodology described above.

Bibliography

[1] L. Bachelier, Théorie de la Spéculation, Gauthier-Villars, 1900.

[2] G. Bakshi, C. Cao, Z. Chen, Emperical Performance of Alternative Option Pricing Models, Journal Of Finance, 1997.

[3] O. E. Barndorff-Nielen, Processes of Normal Inverse Gaussian Type, Finance and Stochastics, 2, 1998.

[4] Bank of International Settlements, Triennial and Regular OTC Derivatives Market Statistics, 2007.

[5] D. Bates, Testing Option Pricing Models, Statistical Methods in Finance, Chapter 20, 1996.

[6] F. Black and M. Scholes, The Pricing of Options and Corporate Liabilities, Journal of Political Economy 81, 1973.

[7] J. Bertoin, Lévy Processes, Second Edition, Cambridge University Press, Cambridge, 1998

[8] T. Bjork, Arbitrage Theory in Continuous Time (2nd Edition), Oxford University Press, 2004.

[9] T. Bollerslev, J. Litvinova and G. Tauchen, Leverage and Volatility Feedback Effects in High-Frequency Data, Journal of Financial Econometrics, Vol. 4, 2006.

[10] P. Carr, H. Geman, D. Madan, M. Yor, Fine Structure of Asset Returns: An Empirical Investigation, The Journal of Business, 2002.

[11] P. Carr, D. Madan, Towards a Theory of Volatility Trading, In Volatility, Pages 417-427, Risk Publications.

[12] P. Carr and D. Madan, Option Pricing and the Fast Fourier Transform, Journal of Computational Finance, 1999.

[13] P. Carr, D. Madan, E. Chang, The Variance Gamma Process and Option Pricing, European Finance Review, 1998.

[14] P. Carr, H Geman, D. Madan and M. Yor, From Local Volatility to Local Levy Models. Quantitative Finance, Vol. 4, 2004.

[15] P. Carr, H Geman, D. Madan and M. Yor, Self Decomposability in Option Pricing, Mathematical Finance 7, 2007

[16] P. Carr and D. Madan, Optimal Positioning in Derivative Securities, Quantitative Finance, 2001.

[17] P. Carr, H Geman, D. Madan and M. Yor, Pricing Options on Realized Variance, Finance and Stochastics, 2005.

[18] R. Cont, P. Tankov, Financial Modelling with Jump Processes, Chapman & Hall/CRC, 2003.

[19] R. Cont, E. Voltchkova, Integro-differential Equations for Option Prices in Exponential Lévy models, Finance and Stochastics 9, 2005.

[20] F. Delbaen, W. Schachermayer, The Variance-Optimal Martingale Measure for Continuous Processes, Bernoulli 2 (1996).

[21] E. Derman, I. Kani, and M. Kamal, Trading and Hedging Local Volatility, Journal of Financial Engineering, 1997.

[22] E. Derman, I. Kani, Riding on a Smile, Risk 7, 1994.

[23] B. Dupire, A Unified Theory of Volatility, Derivatives Pricing: The Classic Collection (Editor P. Carr), Risk Books, 2004.

[24] E. Eberlein, U. Keller and K. Prause, New Insight into Smile, Mispricing and Value at Risk: The Hyperbolic Model, Journal of Business, 71, 1998.

[25] E. Eberlein, D. Madan, Sato Processes and the Valuation of Structured Products. FDM-Preprint Nr. 95, University of Freiburg, 2006.

[26] J. Fouque, G. Papanicolaou, K. Sircar, Derivatives in Financial Markets with Stochastic Volatility, Cambridge University Press, 2000.

[27] J. Gatheral, The Volatility Surface: A Practitioner's Guide, Wiley Finance, 2006.

[28] P. Hagan, D. Kumar, A. Leseniewski, D. Woodward, Managing Smile Risk, BNP Paribas Working Papers. http://www.math.columbia.edu/~lrb/sabrAll.pdf

[29] J. Harrison and D. Kreps, Martingale and Arbitrage in Multiperiod Securities Markets, Journal of Economic Theory, 20, 1979.

[30] J. Harrison and S. Pliska, Martingale and Stochastic Integrals in the Theory of Continuous Trading, Stochastic Processes and Their Applications, 11, 1981.

[31] S. Heston, A closed Form Solution for Options with Stochastic Volatility, with Applications to Bond and Currency Options, Review of Financial Studies 6, 1993.

[32] J. Hull, Options, Futures and Other Derivatives (6th Edition), Prentice Hall, 2005.

[33] A. Javaheri, Inside Volatility Arbitrage : The Secrets of Skewness, Wiley, 2005.

[34] S. Kou, A Jump-Diffusion Model for Option Pricing, Working Paper, Columbia University, AFA New Orleans Meetings, 2001.

[35] Available at SSRN: http://ssrn.com/abstract=242367 or DOI: 10.2139/ssrn.10.2139/ssrn.242367

[36] A. Lewis, Option Valuation Under Stochastic Volatility: With Mathematica Code, Finance Press, 2000.

[37] D. Madan, A Tale of Two Volatilities, Submitted to Risk Magazine, 2007.

[38] D. Madan, F. Milne, Option Pricing with V. G. Martingale Components, Mathematical Finance, Vol. 1, 1991.

[39] D. Madan, E. Seneta, The Variance Gamma (V.G.) Model for Share Market Returns, Journal of Business, 1990.

[40] A. M. Matache, C. Schwab and T. P. Wihler, Fast Numerical Solution of Parabolic Integro-Differential Equations with Applications in Finance, SIAM J. Sci. Comput., Vol. 27, No. 2, 2005.

[41] A. M. Matache, T. von Petersdorff, C. Schwab, Fast deterministic pricing of options on Lévy driven assets. M2AN Math. Model. Numer. Anal. 38, 2004.

[42] A. Matacz, M. Potters, The Leverage Effect in Financial Markets: Retarded Volatility, http://www.science-finance.fr/papers/0101120.ps

[43] R. Merton, Theory of Rational Option Pricing, Bell Journal of Economics and Management Science 4, 1973.

[44] R. Merton, Option Pricing When Underlying Stock Returns are Discontinuous, Journal of Financial Economics, 3, 1976.

[45] M. Musiela and M. Rutkowski, Martingale Methods in Financial Modelling, Springer, 2002.

[46] B. Oksendal, Stochastic Differential Equations, Springer, 1998.

[47] T. von Petersdorff and C. Schwab, Wavelet-Discretizations of Parabolic Integro Differential Equations, SIAM J. of Numer. Anal. 2003.

[48] T. von Petersdorff and C. Schwab, Numerical Solution of Parabolic Equations in High Dimensions. M2AN Math. Model. Numer. Anal. 38, 2004.

[49] P. Protter, Stochastic Integration and Differential Equations, Second Edition, Springer-Verlag, Heidelberg, 2005.

[50] K. Sato, Lévy Processes and Infinitely Divisible Distributions, Cambridge University Press, Cambridge, 1999.

[51] W. Schoutens, Levy Processes in Finance: Pricing Financial Derivativesm Wiley Series in Probability and Statistics, 2003.

[52] C. Schwab, Variable Order Composite Quadrature for Singular and Nearly Singular Intervals, Computing, 1994.

[53] J. Yu, On Leverage in a Stochastic Volatility model. J. Econometrics. v127, 2004.

[54] D. Braess, Finite Elements, Second Edition, Cambridge University Press, 2001.

[55] V. Thomée, Galerkin finite element methods for parabolic problems, Springer Series in Computational Mathematics, 1997.

[56] The New CBOE Volatility Index - VIX, 2003, http://www.cboe.com/micro/vix/vixwhite.pdf